REALIZATION OF ALL-PASS TRANSFER FUNCTIONS USING OPERATIONAL AMPLIFIERS AND RLC ELEMENTS

Stefano Romanelli

A MAJOR TECHNICAL REPORT

in the

Faculty

of

Engineering

Presented in partial fulfilment of the requirements for
the Degree of Master of Engineering at
Sir George Williams University
Montreal, Canada

November, 1973

TABLE OF CONTENTS

LIST OF FIGURES

LIST OF TABLES

ABSTRACT

Active all-pass circuits have been known since the early 1930's in their equivalent vacuum-tube versions, yet they never seemed to find practical applications because of the previous cheaper cost and better reliability of the classical passive constant-resistance networks. With the discovery of the transistor and the subsequent introduction of differential operational amplifiers having improved characteristics and excellent low prices, a great quantity of work has been accomplished in the past few years for the realization of "All-Pass Transfer Functions" using operational amplifiers and RC or RCL elements.

It is well known that group delay response, liable to be introduced in a system by cables, amplifiers, etc., must be compensated for by cascading "All-Pass Networks" (normally of second order) having a complementary delay frequency response. The realization of each second order all-pass network requires four and two inductors for its balanced and unbalanced versions respectively. Also, at relatively low frequencies, large amplitude distortions are introduced in the system response by the inductors limited by quality factors. This amplitude distortion must be subsequently compensated by "Amplitude Equalizers".

In this report we shall demonstrate that active all-pass networks exhibiting very flat amplitude response and incorporating the required delay or phase characteristics can be realized, using operational amplifiers, with superior performance and lower cost than their passive equivalents. An active

all-pass network is first derived from its passive lattice equivalent circuit using RLC elements. The inductors are later simulated through gyrators and capacitors. Experimental results are included comparing performance with and without minimum sensitivity design with respect to the operational amplifier gain. An all-pass transfer function with real or complex poles and zeros is realized using a single operational amplifier and RC elements, and the effects of using isolation amplifiers between sections is also shown. Practical limitations, such as the effect of source impedance, finite operational amplifiers gain-bandwidth product, and dissipation present in tuned LC-circuits, are investigated.

ACKNOWLEDGEMENTS

I am indebted to Dr. B.B.Bhattacharyya for his assistance, guidance, and suggestions during the entire preparation of this technical report.

I am also grateful to Dr. V. Ramachandran and to Dr. M. Swamy through whose teaching I gained my first insight into the theory of active networks. I wish also to thank the "Electrical Engineering Department of Sir George Williams University" and "Bell-Northern Research" through whose cooperative attitude this work was made possible.

CHAPTER 1

LITERATURE SURVEY

1.1 Introduction

The transfer function of a second order all-pass network is given by:

$$Kv(s) = (s^2 - 2dw_n s + w_n^2)/(s^2 + 2dw_n s + w_n^2) \quad (1.1)$$

The poles and zeros of this function are the negative of one another as illustrated by the pole-zero pattern of Fig. 1.1. The most familiar and classical realization of the above function through the years has been by using symmetrical lattices[1] terminated by constant resistances in either their balanced or unbalanced form. In the following pages, some of the active structures[2,3,4,5,6] which can realize the transfer function shown in equation (1.1) are described.

1.2 Yanagisawa Configuration

Yanagisawa's configuration[7] for active filters, using a negative impedance converter of the current inversion type, is given in Fig. 1.2. The open circuit transfer voltage ratio of the network is given by:

$$K_v(s) = \left.\frac{V_2}{V_1}\right|_{I_2=0} = -(Y_{21b}-Y_{21a})/(Y_{22b}-Y_{22a}) \quad (1.2)$$

showing that the NIC controls the zeros as well as the poles of the transfer function Kv(s). Knowing that Y_{22a} and Y_{21a} cannot be synthesized separately, Yanagisawa proposed the use of inverted L sections for networks N_a and N_b, as shown in Fig. 1.3. For this circuit we have:

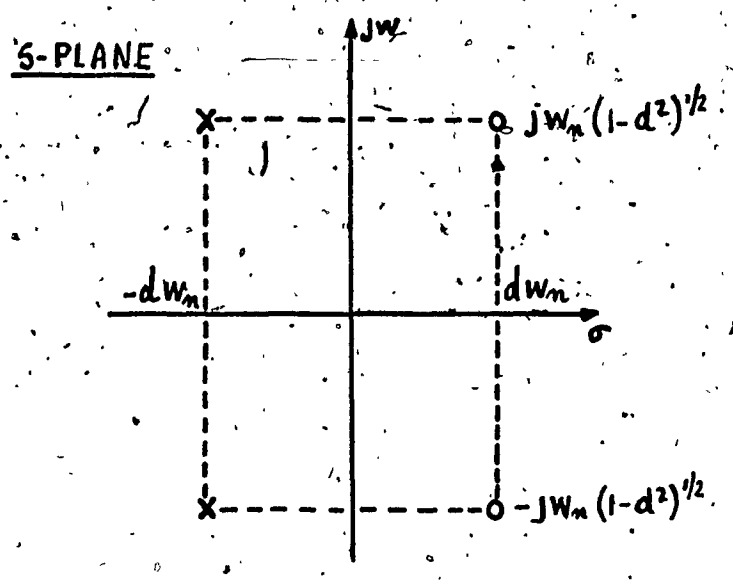

Fig. 1.1 Pole-zero pattern of a second order all-pass section.

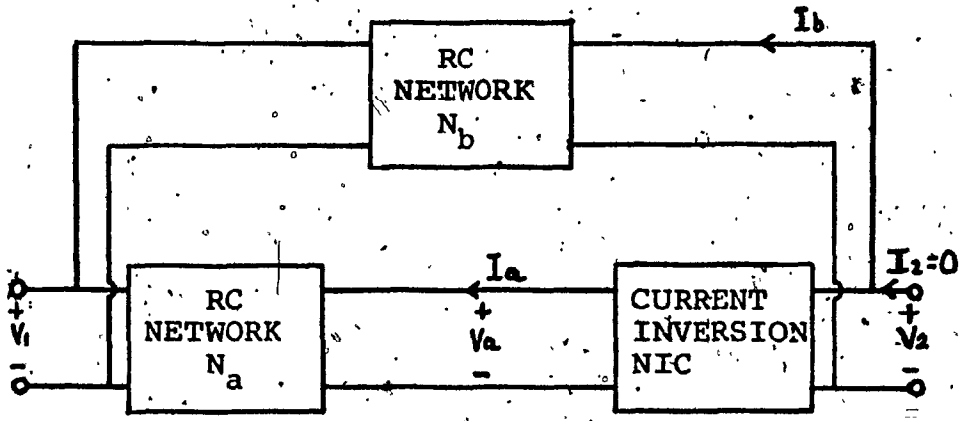

(a)

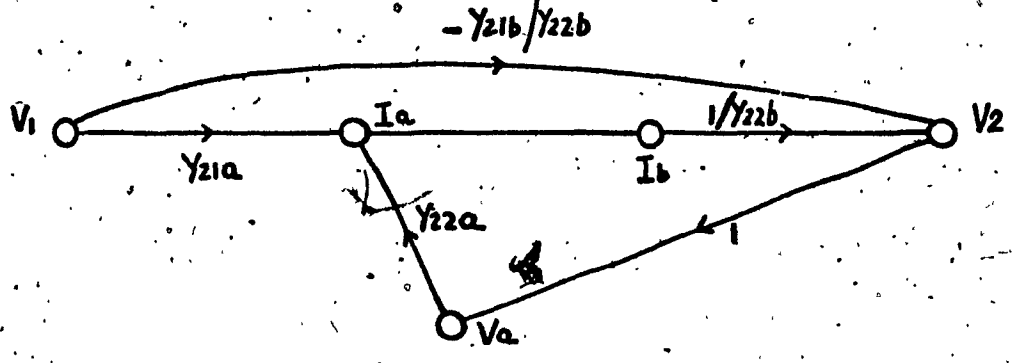

(b)

Fig. 1.2 (a) Yanagisawa's RC-NIC filter
(b) Signal flow graph representation.

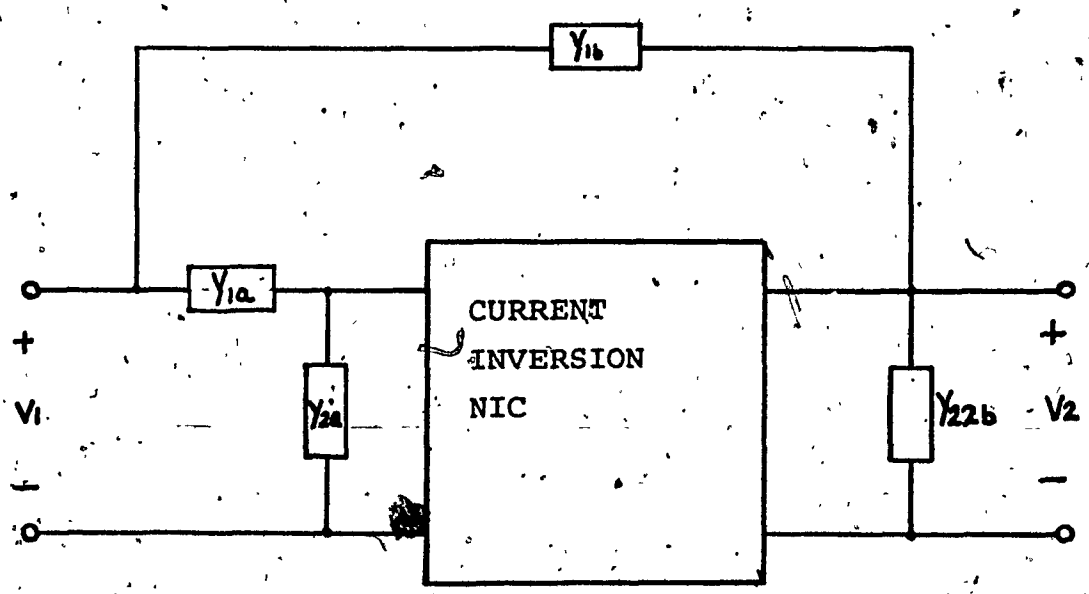

Fig. 1.3 Yanagisawa's filter with inverted L-sections for the two RC network components.

$$K_v(s) = \left.\frac{V_2}{V_1}\right|_{I_2=0} = \frac{Y_{1a}-Y_{1b}}{(Y_{1a}-Y_{1b})+(Y_{2a}-Y_{2b})} \tag{1.3}$$

Writing $K_v(s)$ as

$$K_v(s) = \frac{N(s)}{D(s)} = \frac{N(s)}{N(s)+D(s)-N(s)} \tag{1.4}$$

and dividing the numerator of equation (1.4) by a polynomial $P(s)$ with $m-1$ distinct negative real roots $-a_1,-a_2,\ldots,-a_{m-1}$, where m is the order of $D(s)$, that is:

$$P(s) = \prod_{i=1}^{m-1} (s+a_i) \tag{1.5}$$

we obtain

$$Y_{1a}-Y_{1b} = \frac{N(s)}{P(s)} = k_\infty s + k_o + \sum_{i=1}^{m-1} k_i s/s+a_i \tag{1.6}$$

$$Y_{2a}-Y_{2b} = \frac{D(s)-N(s)}{P(s)} = k'_\infty s + k'_o + \sum_{i=1}^{m-1} k'_i s/s+a_i \tag{1.7}$$

where the partial fraction terms with positive residues and negative residues are realized by Y_{1a}, Y_{2a} and Y_{1b}, Y_{2b} respectively. It should be noted that the structure of Fig.1.3 can accomodate any required physical load simply by adding its admittance to both Y_{2a} and Y_{2b} leaving the complete response unchanged. To realize the all-pass transfer function of equation (1.1) we choose

$$P(s) = s+w_n \tag{1.8}$$

and using equations (1.6) and (1.7) we obtain

$$Y_{1a}-Y_{1b} = \frac{s^2-2dw_n s+w_n^2}{s+w_n} \tag{1.9}$$

$$Y_{2a}-Y_{2b} = \frac{4dw_n s}{s+w_n} \tag{1.10}$$

which gives

$$Y_{2a} = 4dw_n s/s+w_n \tag{1.11}$$

$$Y_{2b} = 0 \tag{1.12}$$

$$Y_{1a} = s + w_n \tag{1.13}$$

$$Y_{1b} = 2w_n(1+d)s/s+w_n \tag{1.14}$$

Equations (1.11) to (1.14) yield the realization shown in Fig. 1.4 with:

$R_1 = 1/w_n$

$C_1 = 1$

$R_2 = 1/2w_n(1+d)$

$C_2 = 2(1+d)$

$R_3 = 1/4dw_n$

$C_3 = 4d$

1.3 Realization Using Two Operational Amplifiers

Let's consider the structure proposed by Lovering[8] shown in Fig. 1.5. Summing the currents at the amplifiers inputs we obtain:

$$Y_1V_1 + Y_3V_a + Y_4V_2 = 0 \tag{1.15}$$

$$Y_2V_1 + Y_5V_a + Y_6V_2 = 0 \tag{1.16}$$

and choosing $Y_3 = Y_5$ and eliminating V_a we get

$$K_v(s) = \frac{V_2}{V_1} = \frac{Y_1 - Y_2}{Y_6 - Y_4} \tag{1.17}$$

Letting $Kv(s) = N(s)/D(s)$ and dividing the numerator and denominator by the auxiliary polynomial $P(s)$ having $m-1$ real roots $-a_1, -a_2, \ldots, -a_{m-1}$, where m is the order of $N(s)$ or $D(s)$, whichever is greater, we can then identify

$$Y_1 - Y_2 = N(s)/P(s) = k_\infty s + k_0 + \sum_{i=1}^{m-1} k_i s/s+a_i \tag{1.18}$$

$$Y_6 - Y_4 = D(s)/P(s) = k'_\infty s + k'_0 + \sum_{i=1}^{m-1} k'_i s/s+a_i \tag{1.19}$$

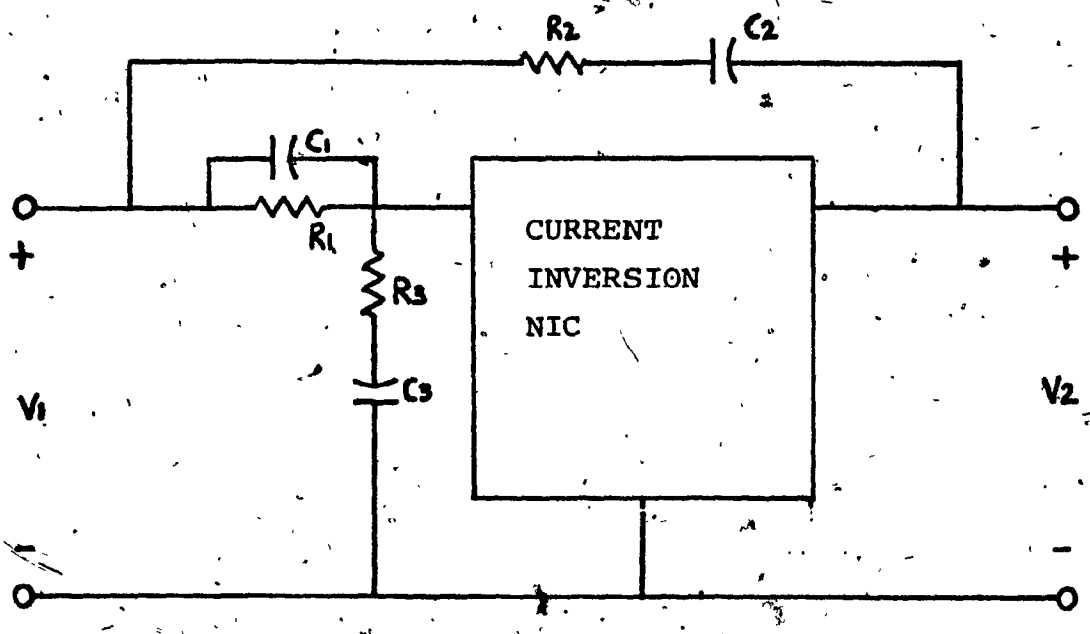

Fig. 1.4 Yanagisawa's second order all-pass section.

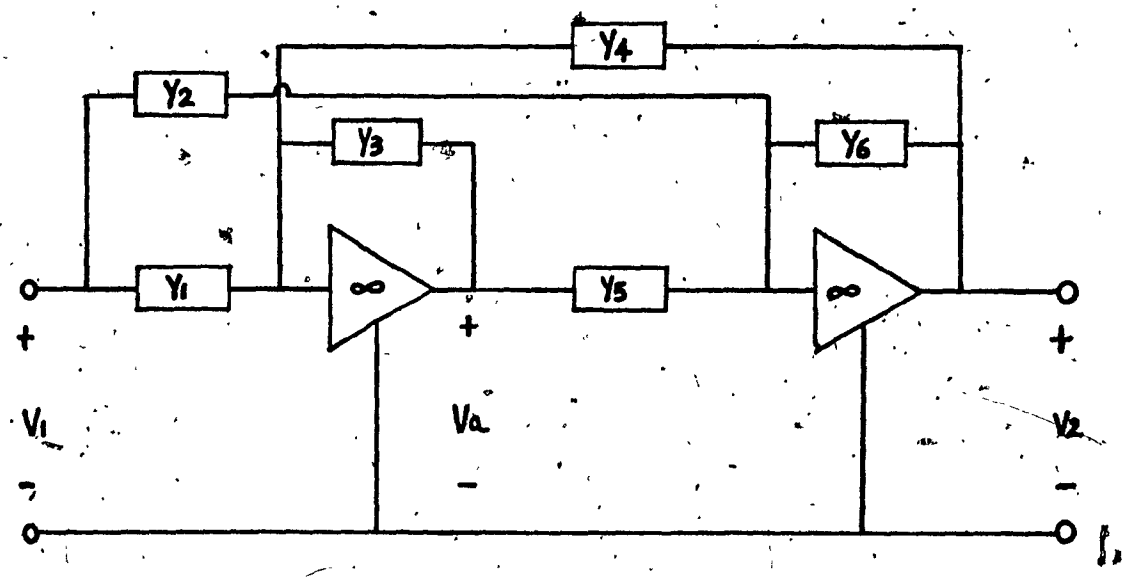

Fig. 1.5 Lovering second order all-pass realization using two opefational amplifiers.

Here, as with Yanagisawa's RC-NIC synthesis procedure, the partial fraction terms with positive residues and negative residues are realized by Y_1, Y_6 and Y_2, Y_4 respectively. To realize the all-pass transfer function of equation (1.1) with $d<1$, we choose

$$P(s) = s + w_n \tag{1.20}$$

obtaining

$$Y_1 - Y_2 = \left[s+w_n\right] - 2w_n s(1+d)/s+w_n \tag{1.21}$$

$$Y_6 - Y_4 = \left[s+w_n\right] - 2w_n s(1-d)/s+w_n \tag{1.22}$$

$$Y_1 = Y_6 = s+w_n \tag{1.23}$$

$$Y_2 = 2w_n s(1+d)/s+w_n \tag{1.24}$$

$$Y_4 = 2w_n s(1-d)/s+w_n \tag{1.25}$$

These values result in the circuit of Fig. 1.6, where:

$$R_1 = R_6 = 1/w_n$$

$$C_1 = C_6 = R_3 = R_5 = 1$$

$$C_2 = 2(1+d)$$

$$R_2 = 1/2w_n(1+d)$$

$$C_4 = 2(1-d)$$

$$R_4 = 1/2w_n(1-d)$$

1.4 Bobrov Realization[9] Using Two Operational Amplifiers

Let's consider the structure shown in Fig. 1.7. The transfer function of this circuit is:

$$K_v(s) = \frac{N(s)/Q(s)}{D(s)/Q(s)} = (Y_3 - \mu Y_4)/(Y_1+Y_3+Y_4-[\alpha-1]Y_2) \tag{1.26}$$

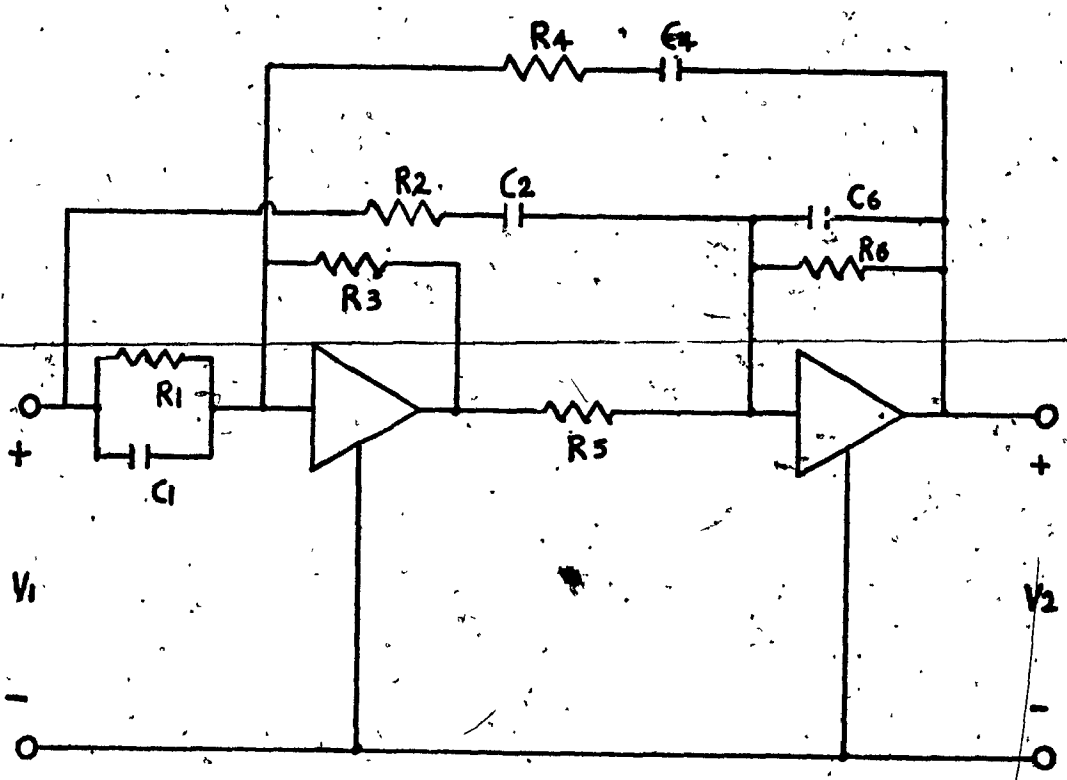

Fig. 1.6 Lovering's second order all-pass section.

To realize the all-pass transfer function of equation (1.1) we choose $Q(s)=s+w_n$ yielding

$$K_v(s) = \frac{s+w_n - [2w_n(1+d)s]/s+w_n}{s+w_n - [2w_n(1-d)s]/s+w_n} \qquad (1.27)$$

Making $\mu=1$ and $\alpha=2$ and comparing expressions (1.26) and (1.27) we obtain

$$Y_3 = s+w_n \qquad (1.28)$$

$$Y_4 = 2w_n(1+d)s/s+w_n \qquad (1.29)$$

$$Y_1 = 0 \qquad (1.30)$$

$$Y_2 = 4w_n s/s+w_n \qquad (1.31)$$

To enable compensation for input and load impedances, Y1 can be chosen as a constant which is then added to Y_2. In this structure the poles and zeros can be controlled independently by changing the gains of the amplifiers, and the structures can be cascaded without buffer stages if a non inverting voltage amplifier with very low output impedance is available.

1.5 Synthesis Using Differential Input Amplifiers

Consider the active RC configuration of Fig. 1.8[10]. The transfer function of this circuit is:

$$K_v(s) = \frac{V_2}{V_1} = \frac{Y_A(Y_B+Y_D+Y_F) - Y_B(Y_A+Y_C+Y_E)}{Y_F(Y_A+Y_C+Y_E) - Y_E(Y_B+Y_D+Y_F)} \qquad (1.32)$$

Choosing $$Y_E = Y_D = 0 \qquad (1.33)$$

$$Y_F = Y_B \qquad (1.34)$$

equation (1.32) reduces to the all-pass transfer function:

$$K_v(s) = \frac{Y_A Y_F - Y_B Y_C}{Y_A Y_F + Y_F Y_C} = \frac{Y_F(Y_A-Y_C)}{Y_F(Y_A+Y_C)} \quad \frac{Z_C-Z_A}{Z_C+Z_A} \qquad (1.35)$$

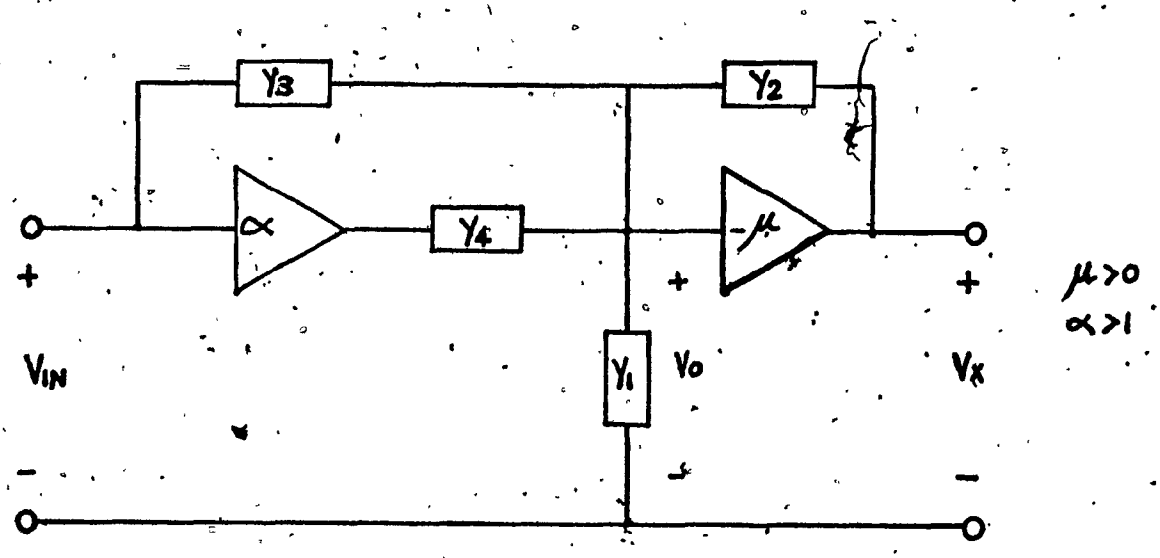

Fig. 1.7 Bobrov two amplifier configuration for voltage transfer ratio realization.

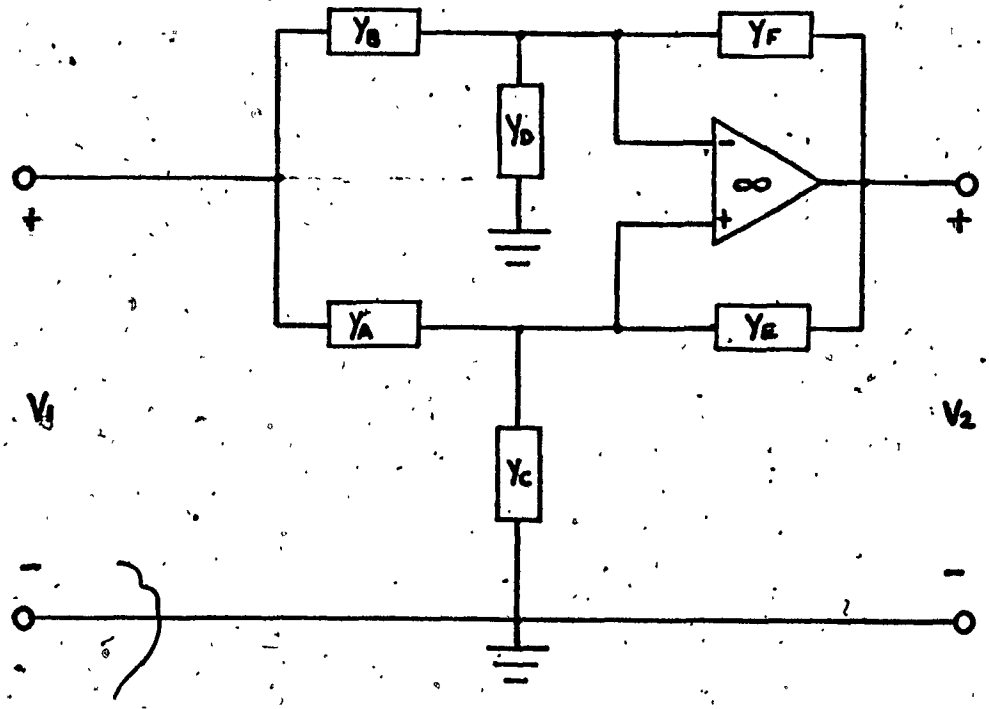

Fig. 1.8 Active RC configuration using a differential input operational amplifier.

Equation (1.35) results in the structure shown in Fig. 1.9. Much more literature is available for the realization of active all-pass networks, most of which deals with realizations using two or more operational amplifiers.

In the following chapter, the one operational amplifier circuits shown in Fig. 1.9 will be analyzed more extensively because of their simplicity and minimum number of components, thus making it more attractive for low quantity production using discrete components. For very large quantities, realizations through integrated circuits would probably be preferred, thus making more feasible the use of more than one operational amplifier to realize each second-order all-pass section.

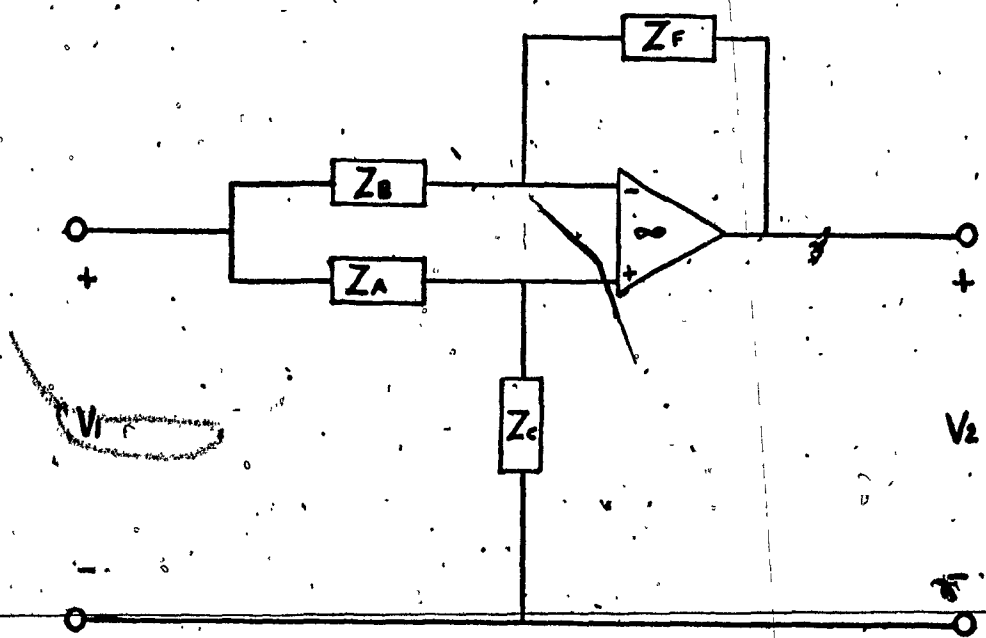

(a)

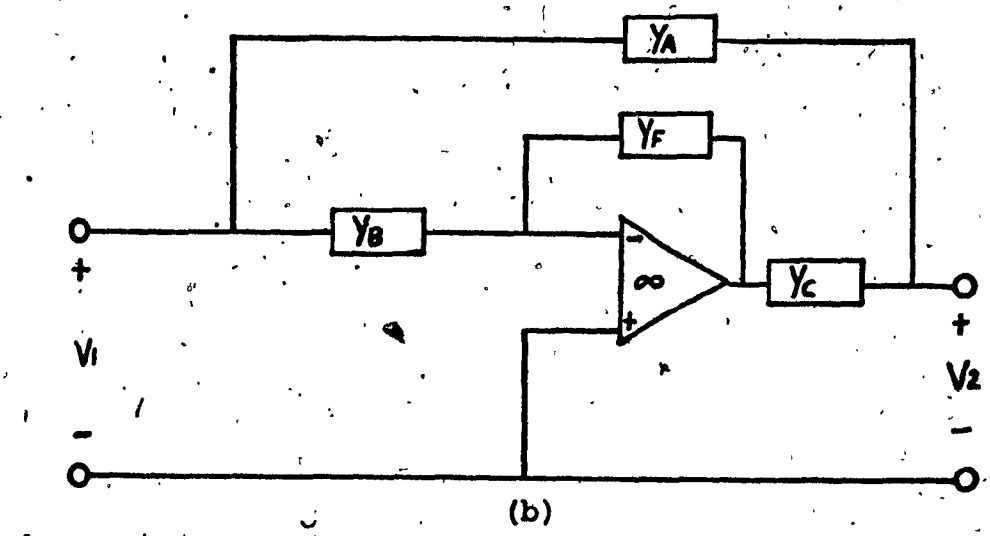

(b)

Fig. 1.9 One operational amplifier all-pass network. (a) Genin's configuration, (b) Bhattacharyya configuration.

CHAPTER 2

SINGLE OPERATIONAL AMPLIFIER ALL-PASS STRUCTURES

2.1 Introduction

It is well known that for a symmetrical lattice, as shown in Fig.2.1, assuming the load resistance is large enough so that the loading is negligible, we have:

$$z_{11} = z_{22} = 1/2\ (Z_A+Z_B) = E_1/I_1 \qquad (2.1a)$$

$$z_{12} = 1/2[\ Z_B-Z_A\ ] = E_2/I_1 \qquad (2.1b)$$

thus

$$E_2/I_1 = (Z_B-Z_A)/(Z_B+Z_A) \qquad (2.1c)$$

Now, if the lattice of Fig.2.1 is terminated by a constant resistance "R", we then get:

$$z_{12} = R\,\frac{(R-Z_A)}{(R+Z_A)} = R\,\frac{(1-(Z_A/R))}{(1+(Z_A/R))} \qquad (2.2)$$

and $Z_AZ_B = R^2$ (2.3)

Under these conditions the input impedance of the cascade connection of any number of lattices is always "R", and if: $|z_{12}(jw)|=R$ for all valuef of "w", then the network has an all-pass behavior.

2.2 One Operatiqnal Amplifier All-Pass Structure

It has been shown[6] that a phase splitter circuit, Fig.2.2, with a Thevenin equivalent as shown in Fig.2.3, will have the transfer function of equation (2.2) under certain conditions. In Fig.2.3, r_1 and r_2 represent the sources impedances and x accounts for differences in the amplifications

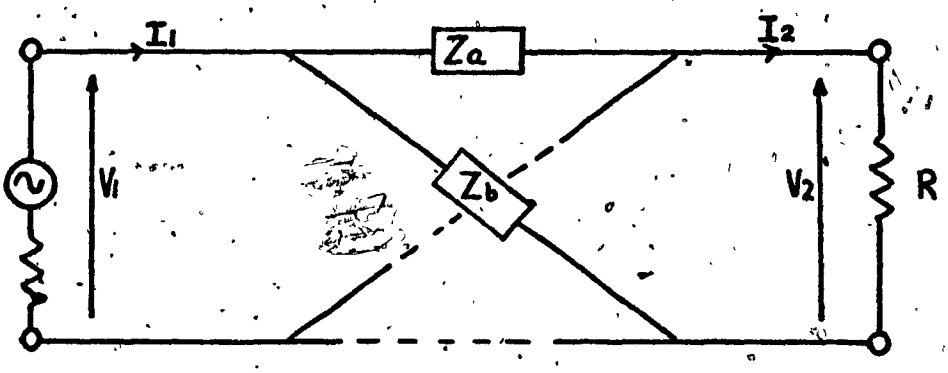

Fig. 2.1 Symmetrical lattice.

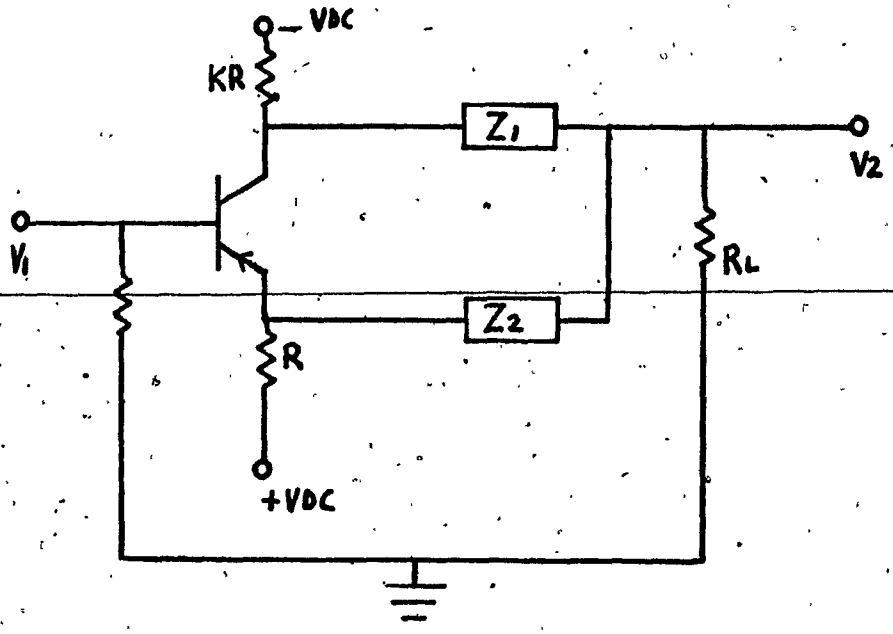

Fig. 2.2 Transistor phase splitter.

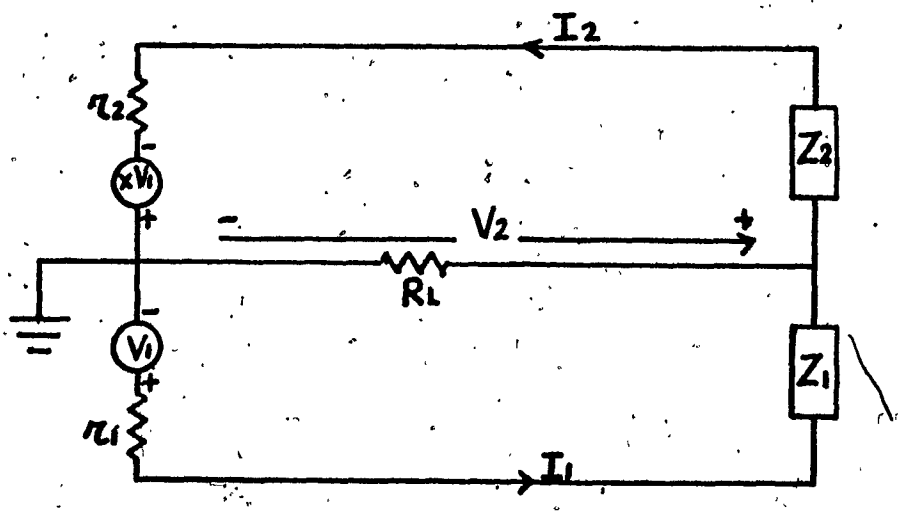

Fig. 2.3 Equivalent circuit of phase splitter.

of the two loops. The transfer function is given by:

$$K_v = \frac{V_2}{V_1} = \frac{R_L}{R_L+R'} \frac{(xR' - r_2) - Z_2}{r_2 + \frac{R'R_L}{R'+R_L} + Z_2} \qquad (2.4)$$

where: $R' = r_1 + Z_1$

Comparing the above equation to equation (2.2), we see that to make the two identical we must have:

$$(x R' - r_2) = r_2 + \frac{R'R_L}{R'+R_L}$$

$$\text{thus: } x = \frac{2r_2}{R'} + \frac{R_L}{R'+R_L} = 1 + \frac{2r_2}{R'} - \frac{R'}{R'+R_L} \qquad (2.5)$$

$$\text{and } R = r_2 + \frac{R'R_L}{R'+R_L} \qquad (2.6)$$

Substituting equations (2.5) and (2.6) into equation (2.4), we finally obtain:

$$K_v = \frac{R_L}{R_L+R'} \frac{R-Z_2}{R+Z_2} = \frac{R_L}{R_L+R'} \frac{1-Z_2/R}{1+Z_2/R} \qquad (2.7)$$

Replacing the transistor in Fig.2.2 by an operational amplifier we obtain the all-pass circuit shown in Fig.2.4. For this circuit, assuming infinite input impedance, zero output impedance, and very high operational amplifier gain, the admittance matrix is:

$$(y) = \begin{bmatrix} Y_1 + \frac{1}{R} & -Y_1 \\ KY_2 - Y_1 & Y_1 + Y_2 \end{bmatrix} \qquad (2.8)$$

and the transfer function is:

$$\frac{V_2}{V_1} = \frac{Y_1 - KY_2}{Y_1 + Y_2} = \frac{1 - KY_2/Y_1}{1 + Y_2/Y_1} \qquad (2.9)$$

which is similar to the previous equations (2.2) and (2.7).

B.B.Bhattacharyya and M.N.S.Swamy[4,11] showed that the all-pass circuit of Fig.2.4 was equivalent to Genin's circuit[3] shown in Fig.2.5 and having the transfer function:

$$\frac{V_2}{V_1} = \frac{1 - KZ_1/Z_2}{1 + Z_1/Z_2} \qquad (2.10)$$

Now, if in Fig.2.1 we assume that Z_A and Z_B are lossless (LC-network with infinite quality factors), then we have:

$$Z_A = R_A + jX_A = jX_A$$

$$Z_B = R_B + jX_B = jX_B$$

thus:

$$\frac{E_2}{E_1} = \frac{I_2}{I_1} = \frac{1}{e^{a+jb}} = \frac{R-jX_A}{R+jX_A} = \frac{jX_B - R}{jX_B + R} \qquad (2.11)$$

The attenuation and envelope delay of equation (2.11) are respectively given by:

$$a = 0$$

$$\tau = \frac{db}{dw} = \frac{2R}{R^2+X_A^2}\frac{dX_A}{dw} = \frac{2R}{R^2+X_B^2}\frac{dX_B}{dw} \qquad (2.12)$$

In practice, because of element losses, the real parts R_A and R_B of Z_A and Z_B are not zero, resulting in a finite attenuation value a varying with frequency.

2.3 DESIGN OF 2nd ORDER ALL-PASS NETWORK USING GENIN'S CIRCUIT

A second order all-pass lattice was first designed as shown in Fig. 2.6, where:

$$w_r L_a = 1/w_r C_a = mR \qquad (2.13)$$

$$w_r L_b = 1/w_r C_b = \frac{1}{m}R \qquad (2.14)$$

m = Steepness factor = 0.2; F_r = 1000 Hz.

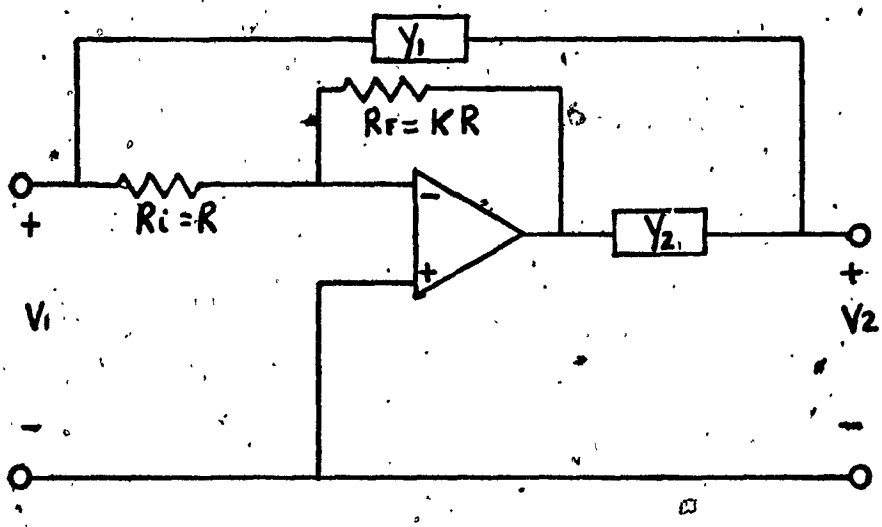

Fig. 2.4 All-pass network using operational amplifiers. "Bhattacharyya configuration"

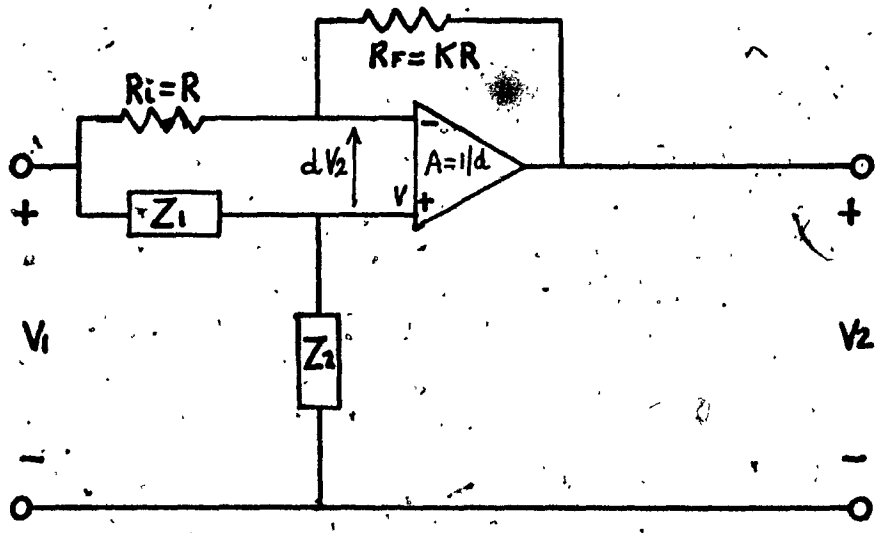

Fig. 2.5 All-pass network using operational amplifiers "Genin's configuration"

This circuit (for m≤1) was next reduced to its unbalanced form, Fig. 2.7, with values:

L_a= 19.0985 mH

L_b= 477.4648 mH

C_a= 1.32629 MF

C_b= .05305 MF

F_r = 1000 Hz; m=0.2; $R_{in}=R_{out}$= 600Ω

and its amplitude and delay responses were obtained using the computer library program "Mesh,Del", available at Northern Electric.

The all-pass active circuit shown in Fig. 2.5, with K=1, and using Fairchild operational amplifier μA741C, was next mounted and its response, measured using the instruments listed in Table 2.1 , is shown in Fig. 2.8 as compared to the passive all-pass lattice results. The parallel LC-configuration was used for Z_2, although the series configuration could have equally been used. The graph shows that the delay responses of the two networks were completely identical while the amplitude responses were closely matched and shifted by approximately 0.4 db. Note that no attempt was made to compensate for the inductor dissipation factor as our present exercise was to simulate the response of the passive circuit as close as possible.

Having proven the equality of the passive and active circuits, we tried to improve the amplitude response. From equation (2.10) we have:

$$\frac{V_2}{V_1} = \frac{1-KZ_1/Z_2}{1+Z_1/Z_2} = \frac{1-(KR_1/(R_2+jX_2))}{1+(R_1/(R_2+jX_2))} \qquad (2.15)$$

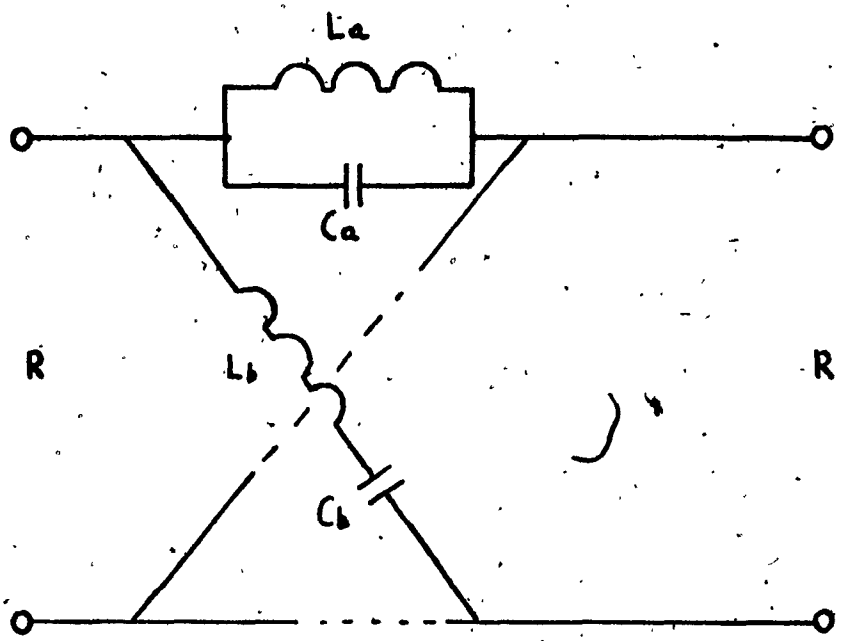

Fig. 2.6 Balanced second order all-pass lattice.

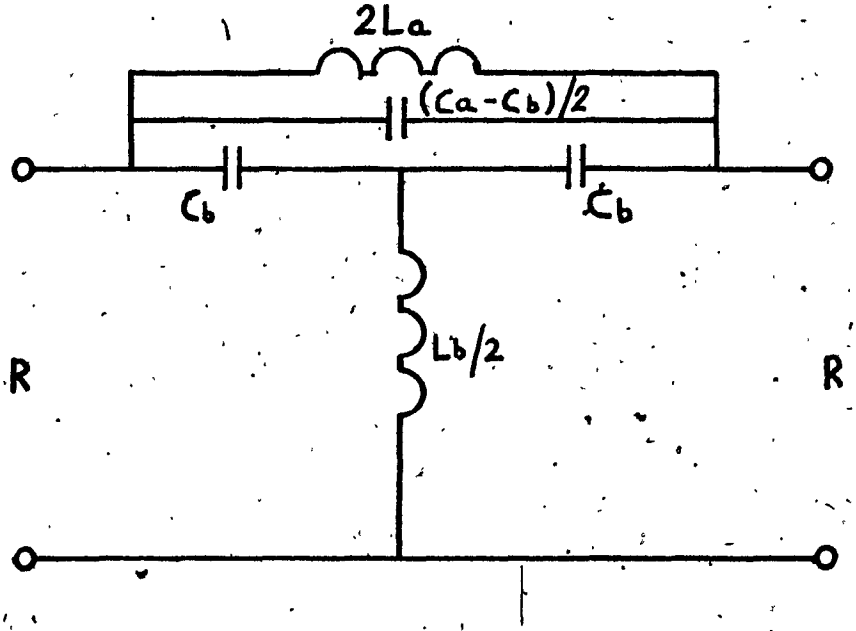

Fig. 2.7 Unbalanced second order all-pass structure.

TABLE 2.1

TESTING AND ADJUSTING EQUIPMENT

1. Delay and Attenuation Measuring Set, Wandel and Goltermann, Model LDS-2 & LDE-2.
2. Frequency Counter, H.P., Model 5321B.
3. Power Supply, Harrison, Model 6206B (2 required)
4. VTVM., H.P., Model 400EL (2 required)
5. Signal Generator, H.P., Model 200CP (600 Ω)

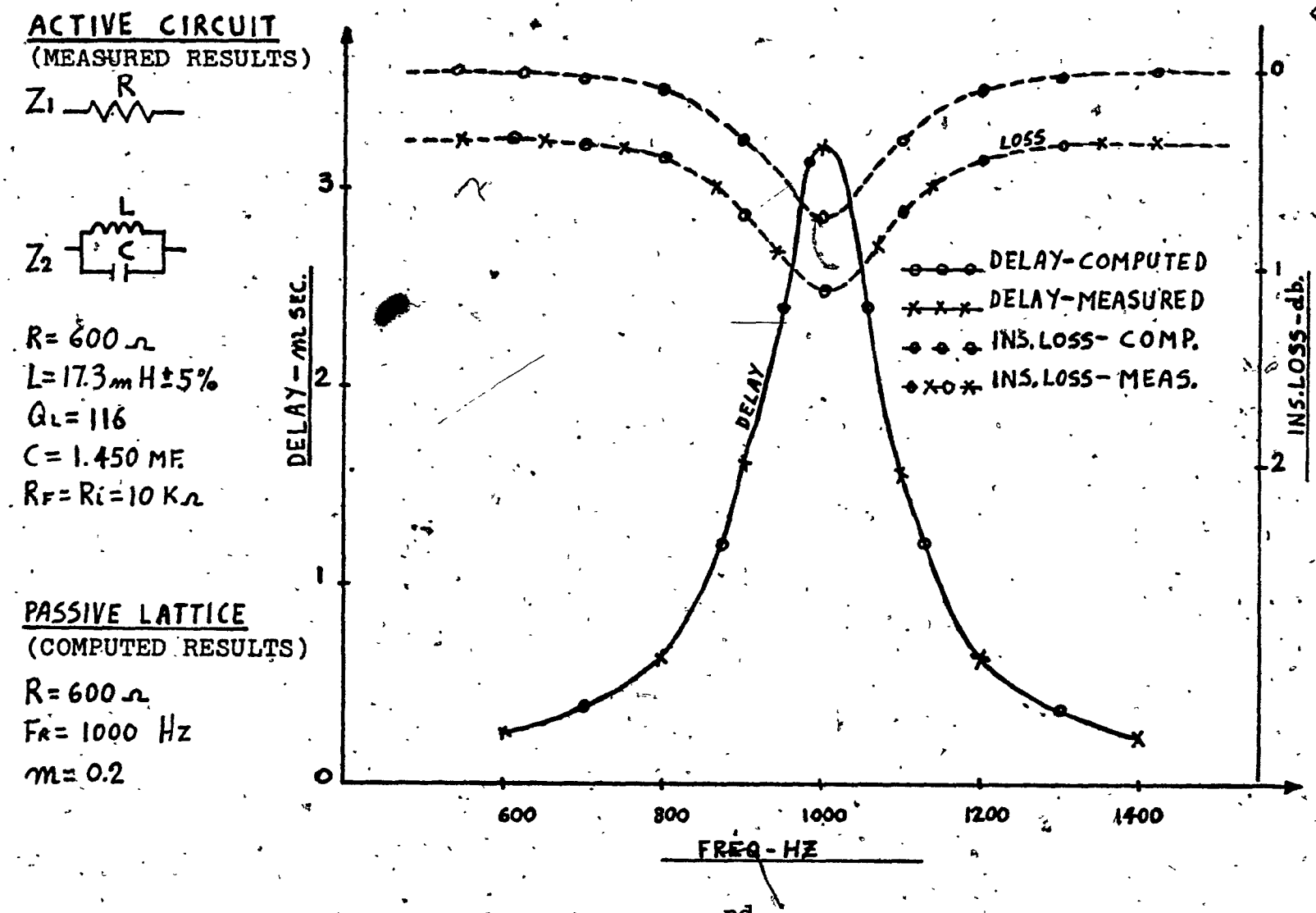

Fig 2.8 Delay and Amplitude responses of 2nd order passive all-pass network and of its active equivalent circuit.

Looking at equation (2.15) we see that to keep the amplitude constant we should have:

$$(1-(KR_1/R_2))/(1+(R_1/R_2)) = -1 \qquad (2.16)$$

where: $R_1 = Z_1$

R_2 = Real part of Z_2 = Inductor effective resistance

and this could be achieved by increasing the gain of our operational amplifier "K".

To prove our point, NE-QHP85 inductors (Q_1=23, R_{ef}=117Ω) were used in our next experiment. Two second-order all-pass networks were cascaded together with center frequencies at 900 Hz. and 1000 Hz.

With R_1= 410Ω, from equation (2.16) we obtained:

$$(1- 410K/117)/(1+ 410/117) = -1 \qquad (2.17)$$

thus: $K = 1.57$.

Two active circuits were next mounted (K=1.7), and their response were measured individually and in cascade, as shown in Fig. 2.9. The computed and measured delay responses agreed very closely, and most important, the compensation allowed in our operational amplifier to offset the inductor dissipation made the amplitude response of the active circuit extremely flat as compared to its passive counterpart which had a 6.5 db. amplitude distortion at the center frequency. Here it should also be noted that no extra operational amplifiers were used in cascading the two second order sections together.

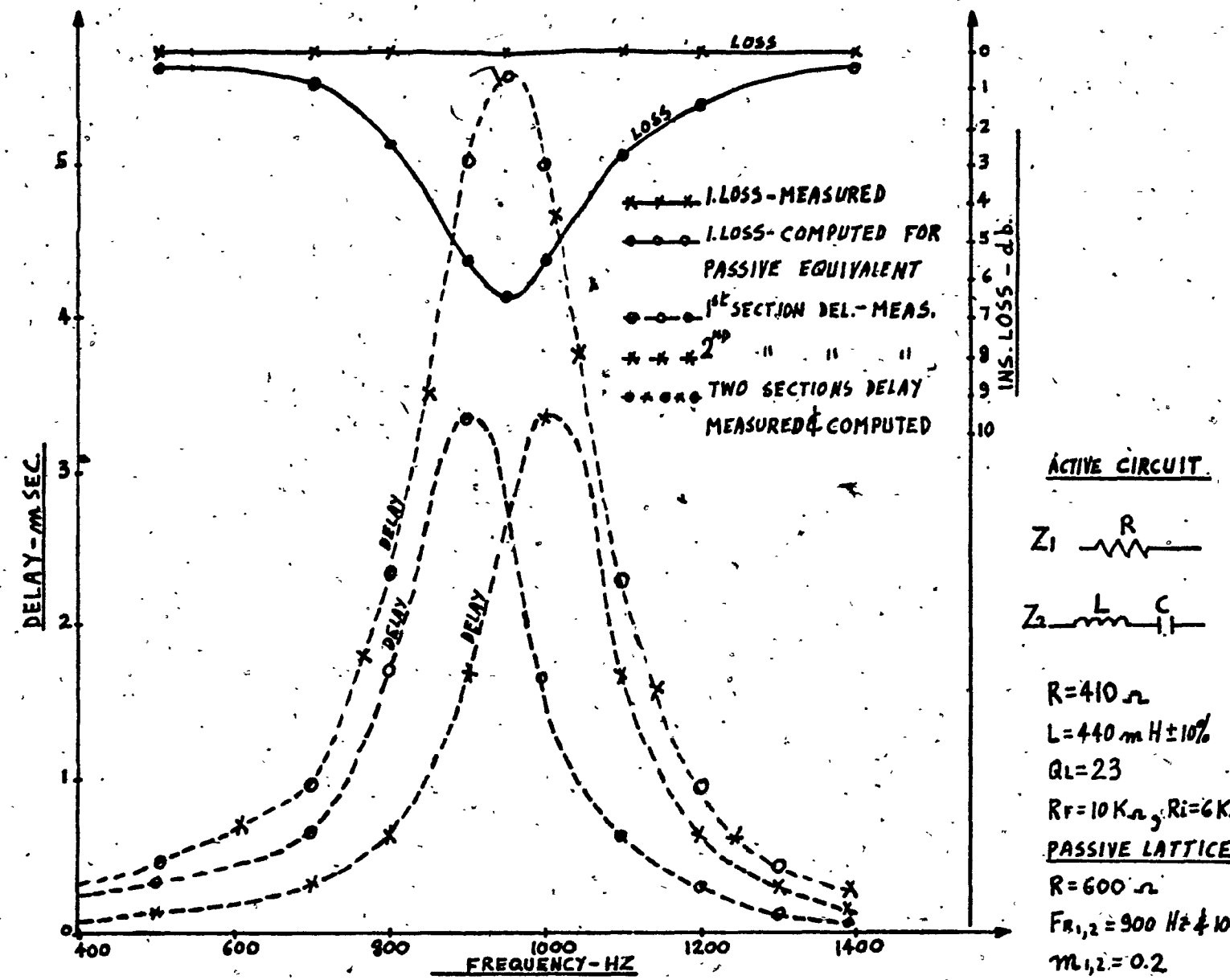

Fig. 2.9 Delay and Amplitude responses of two 2nd order active all-pass networks cascaded together.

2.4 INDUCTORS SIMULATION WITH GYRATORS

Our next step was directed towards replacing the inductors by the use of gyrators. Three main circuit configurations[12,13,14] were investigated and Antoniou's circuit[12], Fig. 2.10, was finally chosen. In this circuit:

a) R_2/R_4 sets the gain

b) For fixed values of "C", the simulated inductance can be varied by changing "R_1".

The components used in our two gyrator circuits were:

$R_2=R_3=R_4=$ 10 K$\Omega\pm$10%

$[C]_1=[C]_2=$ .0127 MF.

$[R_1]_1=$ 200$\Omega\pm$5%

$[R_1]_2=$ 210$\Omega\pm$5%

$[R_A]_1=[R_A]_2=$ 0 Ω

Amplifiers were Fairchild μA741C

VDC= $\pm$ 8.5 Volts

The results obtained from the two cascaded circuits, $K_{1,2}=$ 0.935, are shown in Fig. 2.11. Again the delay response matches the computed response very closely while the amplitude response is still very flat. Also, as seen from the graph, the delay response is absolutely stable over the temperature range 0°C to 50°C, while the amplitude response varies by a tolerable amount, although the temperature coefficients of the passive elements were not matched as ordinary carbon resistors and NE-535GS capacitors were used.

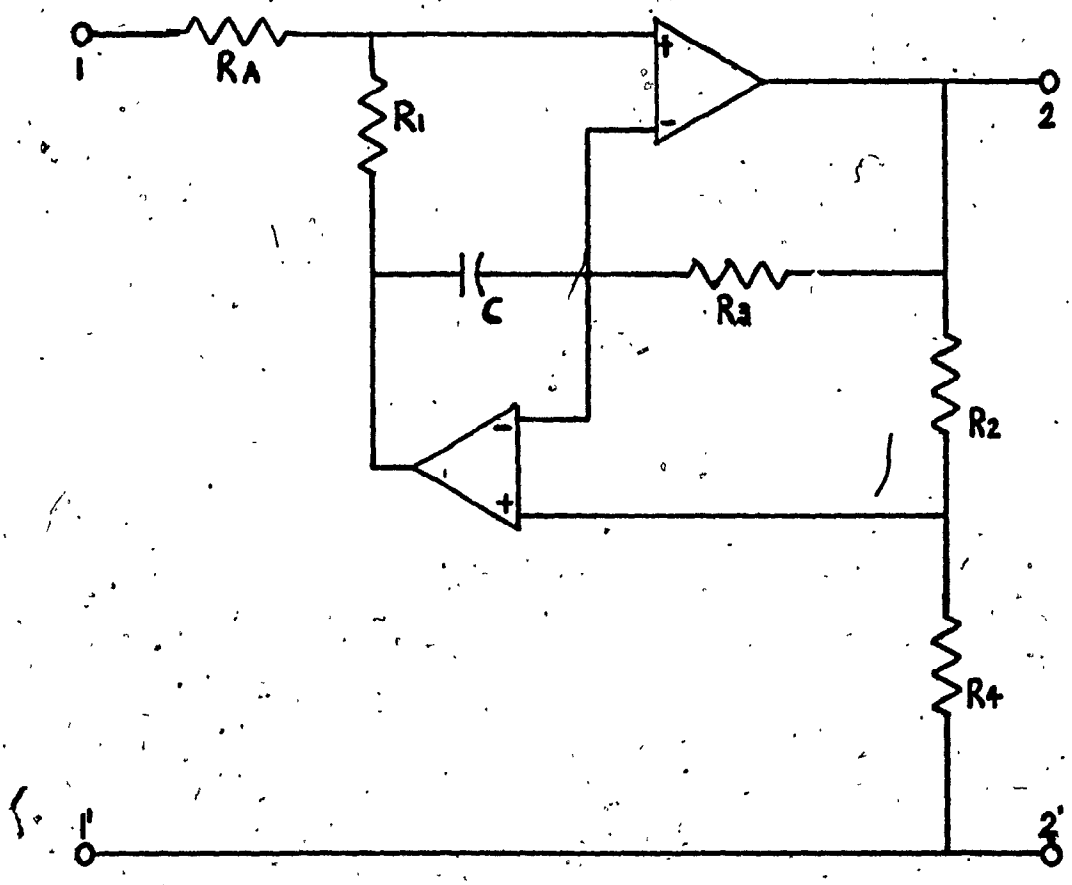

Fig. 2.10 Gyrator terminated by capacitor "C".

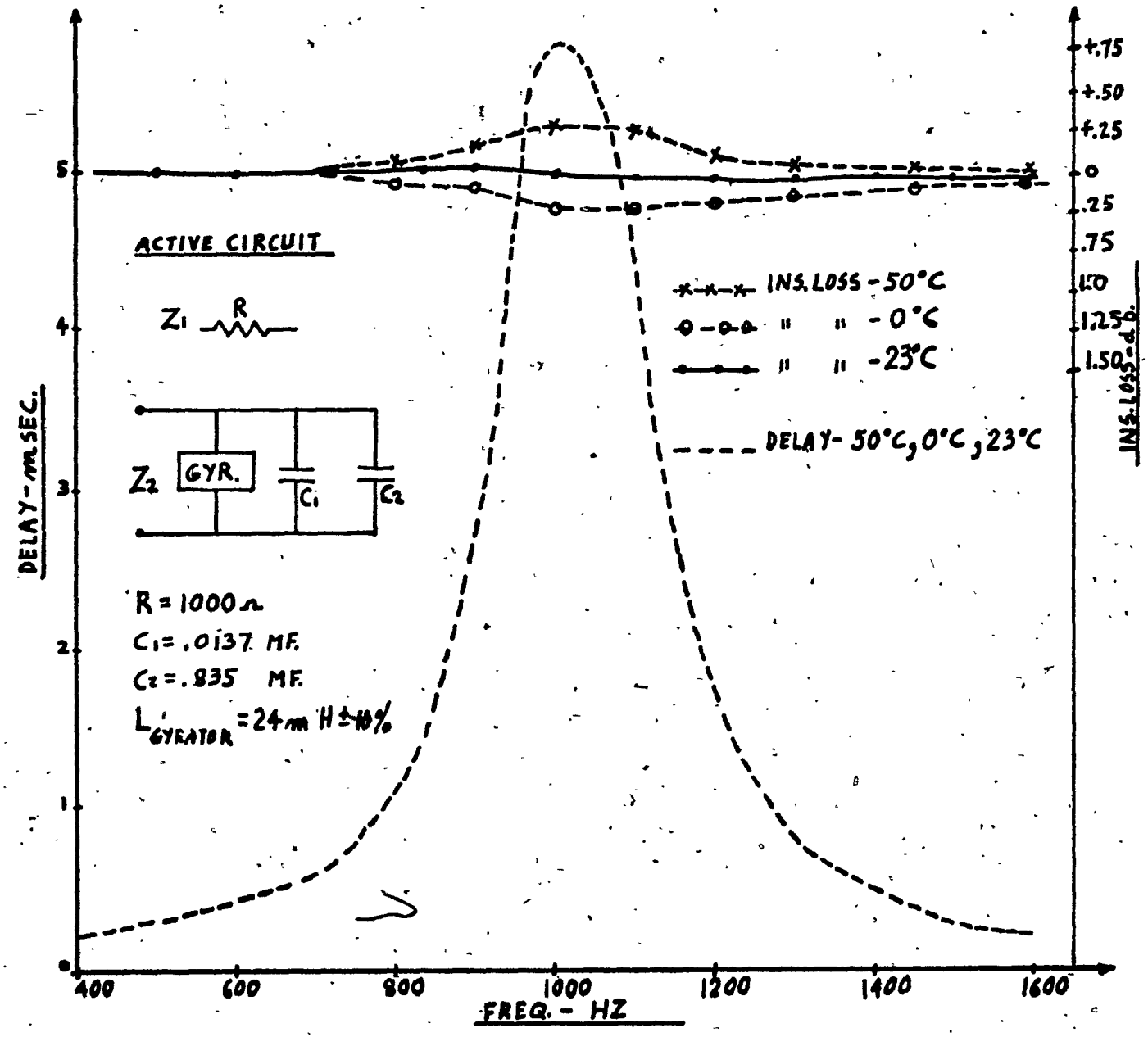

Fig. 2.11 Delay and Amplitude responses of 4th order all-pass network with inductors simulated through gyrators and capacitors.

2.5 DESIGN OF 2nd ORDER ALL-PASS NETWORK USING BHATTACHARYYA CONFIGURATION.

Following the same procedure as explained in the preceeding section, an all-pass structure was realized using Bhattacharyya configuration[4] shown in Fig. 2.4. The results were exactly identical to the ones obtained from Genin's structure, Fig. 2.8.

When two such sections were cascaded without isolation at both ends, errors of approximately 5% and 10% resulted in the overall delay and amplitude responses respectively. This inconvenience was easily eliminated by introducing an isolation amplifier(voltage follower) between the two sections. The transfer function of the voltage follower, Fig. 2.12, is given by:

$$\frac{E_{out}}{E_{in}} = 1/(1+1/A) \qquad (2.18)$$

$$= 1 \qquad (\text{if } A \to \infty)$$

The results were again similar to the previous circuit as shown in Fig. 2.9. Also, as in most practical applications an overall gain is required in the amplitude response so as to compensate for losses present in other system sections, the voltage follower is usually replaced by a non-inverting amplifier, Fig. 2.13, having an overall gain greater than one. The transfer function of this circuit is given by:

$$\text{Gain} = E_{out}/E_{in} = (R_i + R_f)/R_i \qquad (2.19)$$

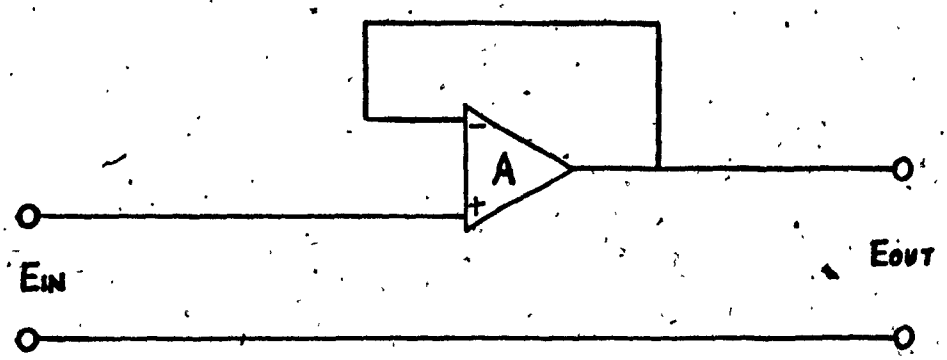

Fig. 2.12 Voltage follower.

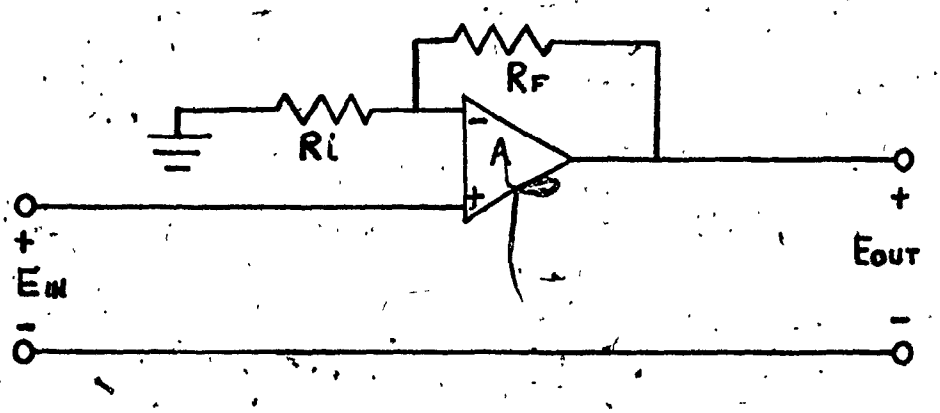

Fig. 2.13 Non-inverting amplifier.

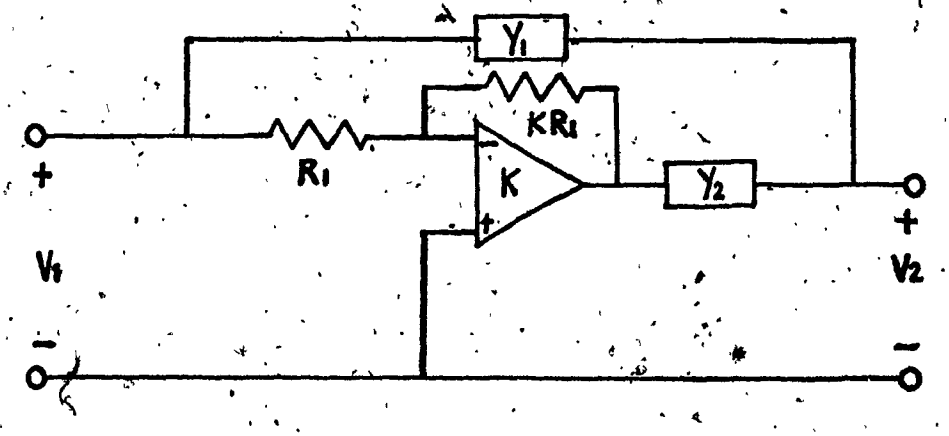

Fig. 2.14 Bhattacharyya all-pass structure.

2.6 ALL-PASS REALIZATION WITH MINIMUM SENSITIVITY DESIGN.

In a recent paper[15], Bhattacharyya and Swamy investigated the realization of the all-pass transfer function:

$$T(s) = \frac{s^2 - (a+b)s + ab}{s^2 + (a+b)s + ab} \qquad a>b>0 \qquad (2.20)$$

using RC-elements, while minimizing the sensitivity of the network function with respect to the amplifier gain"K", Fig.2.14.

Using Horowitz decomposition[16], giving minimum sensitivity with respect to K for the numerator of equation (2.20), the authors obtained:

$$T(s) = \frac{(s+\sqrt{ab})^2 - s(\sqrt{a}+\sqrt{b})^2}{(s+\sqrt{ab})^2 + s(\sqrt{a}-\sqrt{b})^2} \quad ; K=1 \qquad (2.21)$$

Equation (2.21) reduces to:

$$T(s) = \frac{Y_1 + KY_2}{Y_1 + Y_2} \qquad (2.22)$$

by letting:

$$Y_1 = G_1 + sC_1 = \frac{1}{(a)^{1/2} + (b)^{1/2}}(\sqrt{ab} + s) \qquad (2.23a)$$

$$Y_2 = (R_2 + \frac{1}{sC_2})^{-1} = \left\{[\frac{\sqrt{a}+\sqrt{b}}{(\sqrt{a}-\sqrt{b})^2}(1+\frac{\sqrt{ab}}{s})]\right\}^{-1} \qquad (2.23b)$$

$$K = -\left\{[(\sqrt{a}+\sqrt{b})/(\sqrt{a}-\sqrt{b})]\right\}^2 \qquad (2.23c)$$

$$R_1C_1 = R_2C_2 = 1/\sqrt{ab} \qquad (2.23d)$$

A balanced second-order RC-lattice as shown in Fig.2.15 and having the transfer function:

$$T(s) = \frac{(\sqrt{as'})^2 - m\sqrt{as'} + 1}{(\sqrt{as'})^2 + m\sqrt{as'} + 1}, \text{ where } s' \text{ is normalized with respect to } 1/RC. \qquad (2.24)$$

was next designed with:

f_o=1000 Hz.

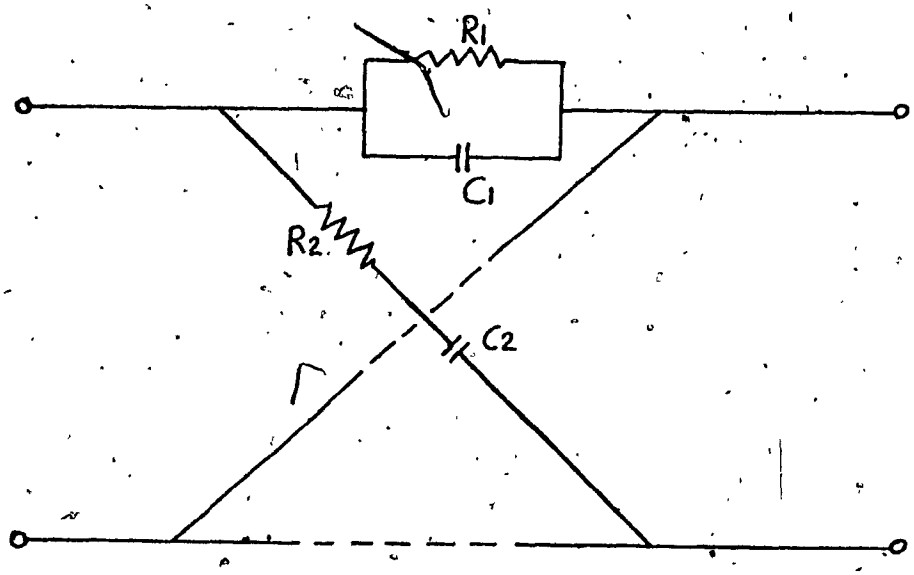

$R_1 = m R/\sqrt{a}$ $\qquad R_2 = R/\sqrt{a}\, m$

$C_1 = C/\sqrt{a}\, m$ $\qquad C_2 = m C/\sqrt{a}$

Fig. 2.15 RC - SECOND ORDER LATTICE - BALANCED FORM.

$a = 1$

$m = 0.7$

$R = \sqrt{10} * 10^4 = 31622.77\ \Omega$

$C = 1/2\pi f_o R = 5032.921210$ Pf.

$w_o CR = 1$

Using R and C we obtain :

$R_1 = mR/\sqrt{a} = 22135.9436\ \Omega$

$C_1 = C/\sqrt{a}\, m = 7189.88744$ Pf.

$R_2 = R/\sqrt{a}\, m = 45175.39514\ \Omega$

$C_2 = mC/\sqrt{a} = 3523.04484$ Pf.

Using the values : $R=31622.7\ \Omega$

$C=5032.9212$ Pf.

$1/CR = 2\pi * 10^3$

in the transfer function:

$$T(s) = \frac{(1-2K) - jK[RCw - (RCw)^{-1}]}{3 + j\,[RCw - (RCw)^{-1}]} \qquad (2.25)$$

or $$T(s) = \frac{K[s^2 + s(1/K+2)(CR)^{-1} + (CR)^{-2}]}{s^2 + 3s(CR)^{-1} + (CR)^{-2}} \quad ; K=-0.2 \qquad (2.26)$$

we obtain:

$$T(s) = \frac{K[s^2 - 6\pi * 10^3 s + (2\pi * 10^3)^2]}{s^2 + 6\pi * 10^3 s + (2\pi * 10^3)^2} \qquad (2.27)$$

Comparing equations (2.26) and (2.20) we see that:

$a+b = 6\pi * 10^3$

$ab = (2\pi * 10^3)^2$

Solving these equations for a and b we get:

$a = 1.644953269 * 10$

$b = 2.399963229 * 10^3$

Feeding these values into equations (2.23a) and (2.23b) we obtain:

$$Y_1 = 35.44905914 + .005641895835\ s$$

$$Y_2 = (2.236071624 + \frac{1.404962675 * 10^4}{s})^{-1}$$

The values obtained to realize Y1 and Y2 are thus:

Y_1: $R_1 = .0282094340\ \Omega$

$C_1 = .005641895835$ Farad

Y_2: $R_2 = 2.236071624\ \Omega$

$C_2 = 7.117626806 * 10^{-5}$ Farad

As the above values were not easily obtainable, they were scaled by a factor of 10^3 resulting in:

$R_1 = 28.2094\ \Omega$

$C_1 = 5.6419$ MF.

$R_2 = 2236.0716\ \Omega$

$C_2 = 71.1763$ NF.

The results obtained from the two above realizations, with Bhattacharyya configuration, Fig. 2.14, are shown in Table 2.2. These results show no apparent differences in the delay response of the two circuits and a more stable response for the "Minimum Sensitivity Circuit" over the temperature range 0° C to 50° C. The two circuits required a long time to adjust and, although resistors with .1% tolerances were used, shunt variable resistors had to be placed across "R" to optimize the responses.

TABLE 2.2

RESULTS FROM ACTIVE ALL PASS NETWORKS DESIGNED WITH AND WITHOUT MINIMUM SENSITIVITY WITH RESPECT TO THE OPERATIONAL AMPLIFIER GAIN.

(B.Bhattacharyya and M.N.S.Swamy Development)

FREQUENCY(Hz.)	DELAY RESPONSE(MICROSECONDS)						
	COMPUTED	MEASURED(WITH MIN. SENSIT.)			MEASURED(WITHOUT MIN. SENS.)		
		23°C	0°C	50°C	23°C	0°C	50°C
200	88.09	88.2	88.2	88.2	88.1	88.1	88.1
400	13.28	13.1	13.1	13.1	13.1	13.1	13.1
600	-49.78	-49.6	-49.6	-49.6	-49.5	-49.5	-49.5
800	-76.46	-76.5	-76.4	-76.6	-76.5	-76.2	-76.9
1000	-71.69	-71.8	-71.6	-72.1	-71.7	-71.2	-72.3
1200	-53.74	-53.8	-53.7	-53.9	-53.6	-53.3	-64.0
1400	-35.57	-35.6	-35.6	-35.6	-35.7	-35.2	-35.7
1600	-21.58	-21.6	-21.6	-21.6	-21.3	-21.2	-21.4
1800	-11.89	-11.9	-11.9	-11.9	-11.6	-11.6	-11.6
2000	- 5.50	- 5.5	- 5.5	- 5.5	- 5.1	- 5.1	- 5.1

CHAPTER 3

PRACTICAL CONSIDERATIONS IN REALIZING ACTIVE DELAY EQUALIZERS.

3.1 Introduction

In this chapter we will consider the limitations present in certain all-pass networks when only RC-elements are used, and the effects introduced in the response of these all-pass networks by: a) Source impedance.
b) Dissipation present in passive elements.
c) Oper. Amplifiers finite gain-bandwidth product.

3.2 Limitations of some active all-pass networks realized using RC elements.

Although it was shown that both Bhattacharyya and Genin configurations, Fig. 2.4 and 2.5, can realize second order all-pass transfer functions using strictly RC elements, the poles and zeros are restricted to real values for finite positive gain values. This is easily seen from their transfer function:

$$TF = \frac{V_2}{V_1} = \frac{1-K(Y_2/Y_1)}{1+(Y_2/Y_1)} = \frac{1-K(Z_1/Z_2)}{1+(Z_1/Z_2)} \qquad (3.1)$$

Letting:

$$Z_1 = R + 1/sC = R + (sC)^{-1}$$

$$\frac{1}{Z_2} = 1/R + sC$$

equation (3.1) becomes:

$$\frac{V_2}{V_1} = \frac{(RCs)^2 + 2RCs - KRCs + 1}{(RCs)^2 + 3RCs + 1} \qquad (3.2)$$

which is all-pass when K = 5. (K = -1/5 if Z1 and Z2 are interchanged).

Equation (3.2) then becomes:

$$\frac{V_2}{V_1} = \frac{(RCs)^2-3RCs+1}{(RCs)^2+3RCs+1} = \frac{s^2\tau^2 - 3\tau s + 1}{s^2\tau^2 + 3\tau s + 1} \qquad (3.3)$$

where: $\tau = RC$

The roots of the numerator of equation (3.3) are:

$$z_{1,2} = \frac{+3\tau \pm (9\tau^2-4\tau^2)^{1/2}}{2\tau^2} \qquad (3.4)$$

The term under the square root sign of equation (3.4) is always positive, thus the roots are restricted to real values. On the contrary, if RLC elements are used, choosing:

$$Z_1 = Ls/1+LCs^2$$

$$Z_2 = R$$

equation (3.1) becomes:

$$\frac{V_2}{V_1} = \frac{R+RLCs^2-KLs}{R+RLCs^2+Ls} \qquad (3.5)$$

which is all-pass when K=1, giving:

$$\frac{V_2}{V_1} = \frac{RLCs^2-Ls+R}{RLCs^2+Ls+R} \qquad (3.6)$$

The roots of the numerator of equation (3.6) are:

$$z_{1,2} = \frac{+L \pm (L^2-4R^2LC)^{1/2}}{2RLC} \qquad (3.7)$$

Here the term under the square root can become negative, thus real and complex roots can be achieved. In practical realizations, this is often required, thus must active all-pass networks are realized using RLC elements, unless the inductor is simulated through a gyrator and a capacitor as was shown in chapter 2.

3.3 Effect of Source Impedance on the Response of an All-Pass Network.

Let's consider the effects of the addition of a finite impedance in series with the source as shown in Fig. 3.1. The transfer function of this circuit is:

$$\frac{V_2}{V_1} = -\frac{R_f}{R_1 + R_s} \quad \frac{Z_1 - R_1R_2/R_f}{Z_1 + R_1(R_2+R_s)/(R_1+R_s)} \tag{3.8}$$

which is an all-pass function when:

$$\frac{R_1R_2}{R_f} = R_1(R_2+ R_s)/(R_1+R_s)$$

i.e.,

$$R_f = R_2(R_1+R_s)/(R_2+R_s) \tag{3.9}$$

Letting $R_1=R_2$, equations (3.8) and (3.9) become:

$$\frac{V_2}{V_1} = -\frac{R_f}{R_1+R_s} \quad \frac{Z1 - R_1(R_2/R_f)}{Z1 + R_1} \tag{3.10}$$

$$R_f = R_2 = R_1 \tag{3.11}$$

Thus, as it can be seen from equation (3.10), the source resistance R_s does not affect the overall response of the all-pass network, except for its effect on the gain of the amplifier.

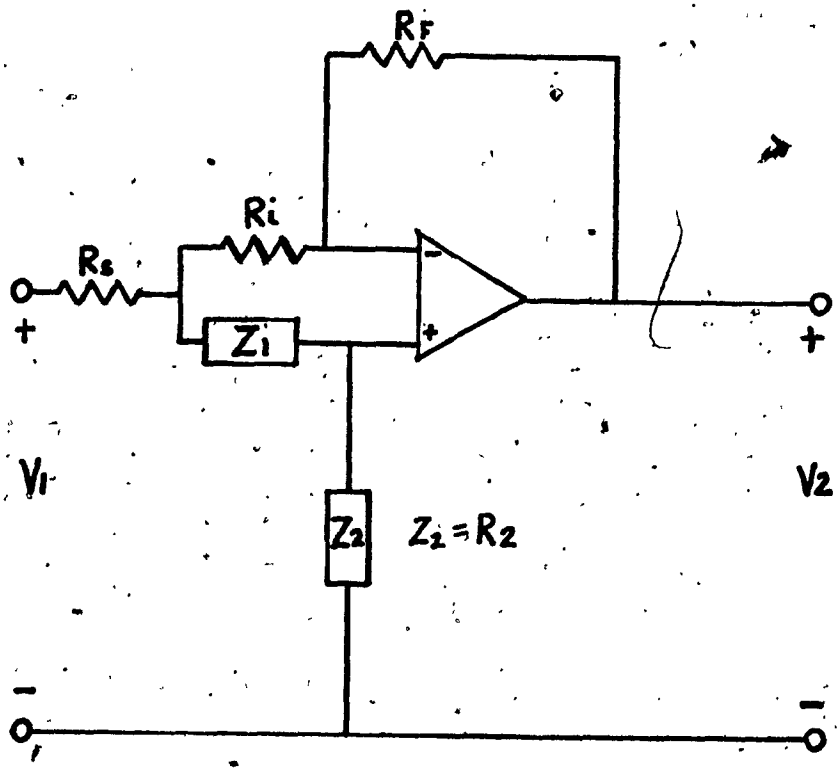

Fig. 3.1 All-pass circuit with source impedance "R_s".

3.4 Compensation of Dissipation Present in Tuned"LC-Circuit" Z1.

Replacing the impedance Z_1 by Z_1+r where r represents the dissipation mainly present in the inductor L equation (3.9) becomes:

$$\frac{R_1R_2}{R_f} - r = \frac{R_i(R_2+R_s)}{(R_i+R_s)} + r = R_o + r$$

i.e.,

$$\frac{1}{R_f} = \frac{R_2+R_s}{R_2(R_i+R_s)} + \frac{2r}{R_i+R_2} \qquad (3.12)$$

Letting $R_2=R_i$, we obtain:

$$\frac{1}{R_f} = \frac{1}{R_2} + \frac{2r}{R_iR_2} = \frac{1}{R_i} + \frac{2r}{(R_i)^2} \qquad (3.13)$$

$$R_o = R_i+r$$

and equation (3.10) becomes:

$$\frac{V_2}{V_1} = -\frac{R_f}{R_i+R_s} \frac{Z_1-R_o}{Z_1+R_o} \qquad (3.14)$$

thus dissipation compensation can be achieved by varying the value of R_f.

3.5 Practical Realization of an Active RLC Delay Equalizer of 8th Order.

For this particular realization the circuit shown in Fig. 3.1 was used with: $Z_2=R_2/\ 1+R_2C_2s$

$$Z_1=L_1s/\ 1+L_1C_1s^2$$

$$R_s=0$$

The single resistor R_2 was here replaced by a parallel combination of " R_2, C_2 " to minimize amplitude deviations above or below the adjusting frequency, thus offsetting the amplifier gain roll-off. Similarly resistors R_f and R_i were paralleled by an extra resistor depending on whether there was respectively gain or loss at the adjusting frequency. The component values used and the measured results are shown in Tables 3.1 and 3.2 respectively. The individual sections were initially adjusted and recorded. Subsequently they were directly cascaded and the overall response was measured. The measurements were taken using the instruments listed in Table 2.1, while the two power supplies were replaced by a single power supply used in conjunction with the "Voltage Divider" shown in Fig. 3.2. Isolation buffer amplifiers were placed at the input and output of the delay equalizer as shown in Fig. 3.3.

3.6 Realization of an Active RC All-Pass Network Applicable to Real or Complex Pole/Zero's Using One Operational Amplifier.

Recently G.E.Roberts [17] investigated an interesting circuit, Fig. 3.4, realizing a second order all-pass transfer function with real or complex poles and zeros by using a second order bandpass resonator and a summing amplifier, pointing a way of adjusting its delay response in the absence of a "Delay Measuring Set-Up". As recent communication equipment call for

TABLE 3.1

ELEMENT VALUES USED IN 8^{th}- ORDER DELAY EQUALIZER.

SECTION	R_f Ω	R_i Ω	L_I H.	QL_I	C_I NF.	R_2 Ω	C_2 PF.	F_o Hz.
1	8070	7500	.128	120	54.2	7500	83.5	1914
2	8045	7500	.101	150	53.6	7500	56.9	2162
3	8095	7500	.0805	150	54.2	7500	52.3	2409
4	8045	7500	.0671	175	53.6	7500	37.9	2654

R's: Vishay with .1% tolerances

C's: N.E. with 1% tolerances

Operational Amplifiers: 741C-MIL

QL: Inductor quality factor at F_o

TABLE 3.2

RESULTS FROM 8th- ORDER RLC DELAY EQUALIZER.

FREQ. Hz.	SECTION-1		SECTION-2		SECTION-3		SECTION-4		TOTAL RESPONSE	
	DELAY msec.	AMP. db.	DELAY msec.	AMP. db.	DELAY msec.	AMP. db.	DELAY msec.	AMP. db.	DELAY msec.	AMP. db.
300	-.03	0	-.014	-.005	-.003	0	0	0	-.047	-.006
500	-.025	0	-.017	0	-.008	0	-.005	0	-.055	0
1000	0	0	0	0	0	0	0	0	0	0
1500	.24	.005	.095	.005	.043	.005	.024	0	.402	.009
2000	1.2	0	1.05	.01	.3	-.01	.12	-.01	2.67	0
2500	.09	.005	.36	0	1.21	0	1.01	-.005	2.66	0
3000	-.03	.01	.03	0.01	.125	-.01	.37	-.005	.498	.005
3500	-.05	.01	-.017	-.01	.014	.015	.056	-.009	-.003	.006
4000	-.06	.015	-.033	-.013	-.01	-.002	.009	.003	-.095	.002
4500	-.07	.005	-.04	.001	-.02	-.005	-.009	0	-.14	0
5000	-.075	0	-.045	0	-.027	.005	-.015	0	-.160	.004

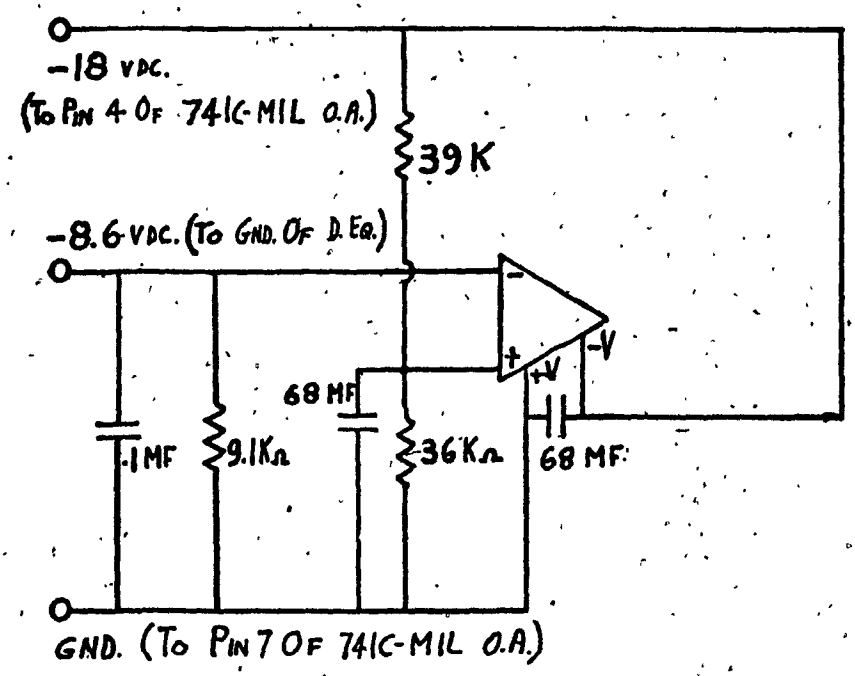

Fig. 3.2 Voltage divider.

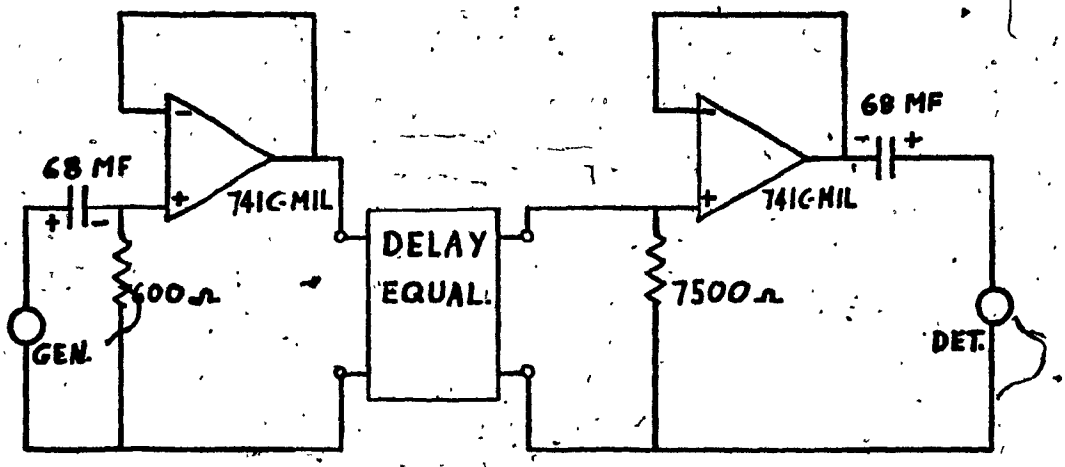

Fig. 3.3 Delay equalizer as tested within isolation buffer amplifiers.

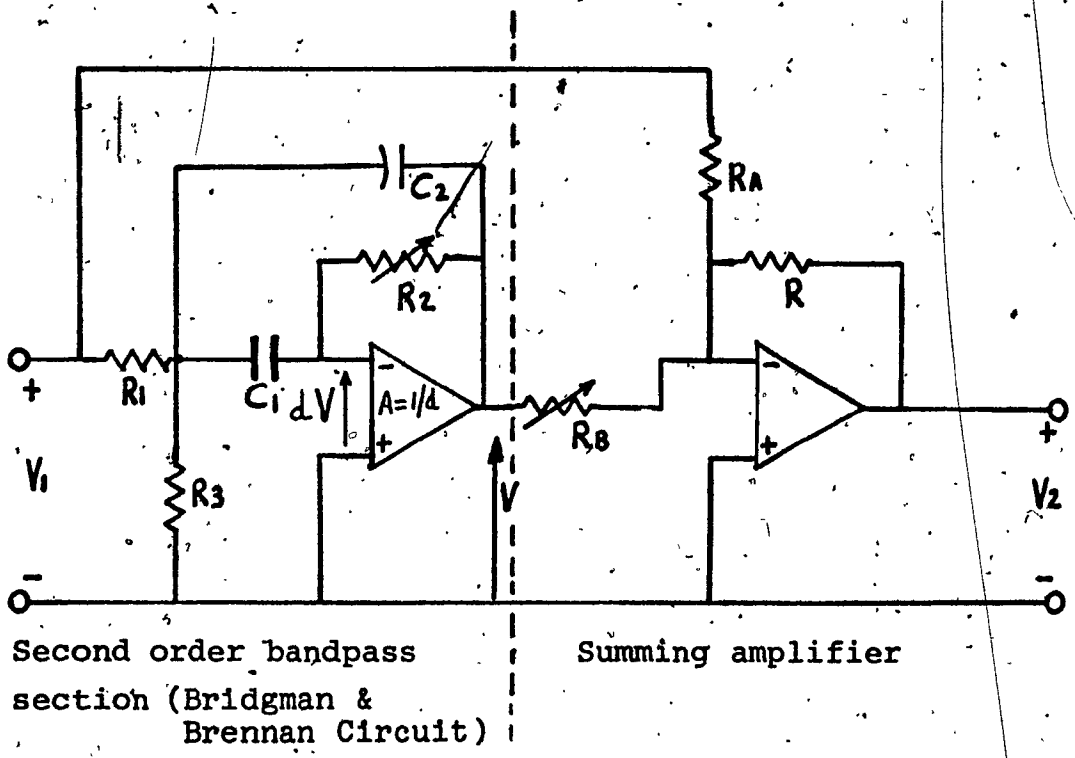

Fig. 3.4 Second order all-pass active RC-network.

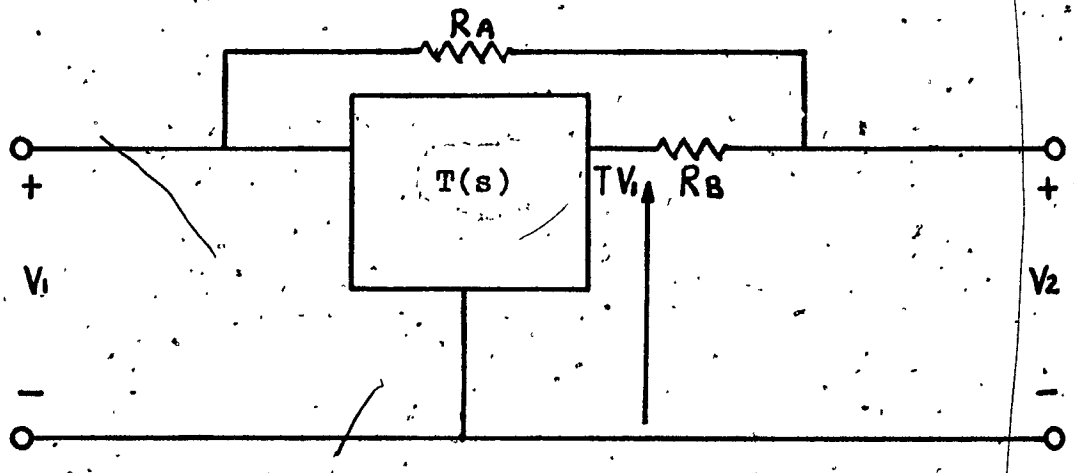

Fig. 3.5 General structure of 2nd order all-pass active RC-network. (Modified Bridgman & Brennan Circuit)

very tight delay equalization(± .05 msec.), making delay measurement practically compulsory, we will modify the circuit so as to realize a second order all-pass function with real or complex poles and zeros using one operational amplifier with the assumption that a delay measuring set-up is available. Analysis of the second order bandpass section of Fig. 3.4, with R3 removed and with the assumption that the gain of the operational amplifier "A=1/d" is taken as "Ax/s+x", where:

A= Open loop-gain at s=0 (dc gain)

x= Unity gain crossover frequency with the open-loop response of the operational amplifier having a -6 db. per octave(-20 db. per decade) roll off rate, gives-

$$i_{R_2}=\frac{V}{R_2}(1+d)=i_{C_1} \tag{3.15}$$

$$i_{C_2}= sC_2\left(\frac{V}{R_2}(1+d)\left(R_2+\frac{1}{sC_1}\right)\right) \tag{3.16}$$

$$-dV=\frac{V}{R_2}(1+d)\,\frac{1}{sC_1} + (i_{C_2} + i_{C_1})R_1+V_1$$

$$-dV=\frac{V}{R_2}(1+d)\frac{1}{sC_1} +\left[sC_2R_1\left\{\frac{V}{R_2}(1+d)\left(R_2+\frac{1}{sC_1}\right)\right\}+\frac{VR_1}{R_2}(1+d)\right]+V_1 \tag{3.17}$$

Thus:

$$V_1=-V\left[d+\frac{1+d}{sC_1R_2} + sC_2R_1(1+d)\frac{sC_1R_2+1}{sC_1R_2} +\frac{R_1}{R_2}(1+d)\right]$$

$$\frac{V}{V_1}= -\frac{sC_1R_2}{s^2C_1C_2R_1R_2(1+d)+s(C_1R_2d+C_2R_1+C_2R_1d+C_1R_1+R_1C_1d)+1+d}$$

$$= -\frac{1}{1+d}\,\frac{sC_1R_2}{s^2C_1C_2R_1R_2+s\left(\frac{C_1R_2d}{1+d}+R_1C_1+C_2R_1\right)+1} \tag{3.18}$$

Assuming $1/1+d \approx 1$, we get:

$$\frac{V}{V_1} = T(s) = -\frac{sC_1R_2}{(s^2/w^2) + s(C_1R_2d + (C_1+C_2)R_1) + 1}$$

$$= -\frac{sC_1R_2}{(\frac{s}{w})^2 + \frac{s}{w}\left[\frac{C_1R_2d}{(C_1C_2R_1R_2)^{1/2}} + \frac{(C_1+C_2)R_1}{(C_1C_2R_1R_2)^{1/2}}\right] + 1} \qquad (3.19)$$

where: $w^2 = 1/C_1C_2R_1R_2$

$$T(s) = -\frac{sC_1R_2}{(\frac{s}{w})^2 + \frac{s}{w}\left[\left(\frac{C_1R_2}{C_2R_1}\right)^{1/2} d + \frac{C_1+C_2}{C_2}\left(\frac{C_2R_1}{C_1R_2}\right)^{1/2}\right] + 1}$$

Letting: $Q = \frac{C_2}{C_1+C_2}\left(\frac{C_1R_2}{C_2R_1}\right)^{1/2}$ and $K = (C_1+C_2)/C_2$,

we get:

$$T(s) = -\frac{sC_1R_2}{(s/w)^2 + (s/w)(QKd + \frac{1}{Q}) + 1} \qquad (3.20)$$

Also, from Fig. 3.5 we obtain:

$$\frac{V_2 - V_1}{R_A} = \frac{TV_1 - V_2}{R_B}$$

$$\frac{V_2}{V_1} = \frac{TR_A + R_B}{R_A + R_B} = T\frac{R_A}{R_A+R_B} + a = \left[\frac{TR_A}{R_B} + 1\right] a \qquad (3.21)$$

where: $a = R_B/R_A + R_B < 1$

Inserting equation (3.20) into equation (3.21) we obtain:

$$\frac{V_2}{V_1} = \left[-\frac{R_A}{R_B}\frac{sC_1R_2}{(s/w)^2 - (s/w)(QKd + \frac{1}{Q}) + 1} + 1\right] a \qquad (3.22)$$

$$= a\frac{(s/w)^2 + (s/w)(QKd + \frac{1}{Q} - C_1R_2R_A/R_B\sqrt{(C_1C_2R_1R_2)}) + 1}{(s/w)^2 + (s/w)(QKd + \frac{1}{Q}) + 1}$$

$$= a\frac{(\frac{s}{w})^2 + \frac{s}{w}\left[QKd + \frac{1}{Q}\sqrt{\frac{C_1R_2}{C_2R_1}}\frac{C_2}{C_1+C_2}\frac{C_1+C_2}{C_2}\frac{R_A+R_B-R_B}{R_B}\right] + 1}{(\frac{s}{w})^2 + \frac{s}{w}(QKd + \frac{1}{Q}) + 1}$$

$$\frac{V_2}{V_1} = a\,\frac{\left(\frac{s}{w}\right)^2+\left[\frac{s}{w}\left\{QKd+\frac{1}{Q}+QK\left(\frac{a-1}{a}\right)\right\}\right]+1}{\left(\frac{s}{w}\right)^2+\frac{s}{w}\left(QKd+\frac{1}{Q}\right)+1} \qquad (3.23)$$

where: $d = \frac{s+x}{Ax} = \frac{s}{Ax} + \frac{1}{A}$

$$\frac{V_2}{V_1} = a\,\frac{\left(\frac{s}{w}\right)^2+\frac{s}{w}\left[\frac{QKsw}{Axw}+\frac{QK}{A}+\frac{1}{Q}+QK\left(\frac{a-1}{a}\right)\right]+1}{\left(\frac{s}{w}\right)^2+\frac{s}{w}\left[\frac{QKsw}{Axw}+\frac{QK}{A}+\frac{1}{Q}\right]+1} \qquad (3.24)$$

$$= a\,\frac{\left(\frac{s}{w}\right)^2\left(1+\frac{QKw}{Ax}\right)+\frac{s}{w}\left[\frac{1}{Q}+QK\left(\frac{1}{A}+\frac{a-1}{a}\right)\right]+1}{\left(\frac{s}{w}\right)^2\left(1+\frac{QKw}{Ax}\right)+\frac{s}{w}\left[\frac{1}{Q}+\frac{QK}{A}\right]+1}$$

Letting $p=s/w$, we obtain:

$$\frac{V_2}{V_1} = a\,\frac{p^2\left(1+\frac{QKw}{Ax}\right)+p\left[\frac{1}{Q}+\frac{QK}{A}+\frac{QK(a-1)}{a}\right]+1}{p^2\left(1+\frac{QKw}{Ax}\right)+p\left(\frac{1}{Q}+\frac{QK}{A}\right)+1} \qquad (3.25)$$

$$= a\,\frac{p^2+p\left(\frac{1}{Q}+\frac{QK}{A}+QK\,\frac{a-1}{a}\right)\frac{1}{B^2}+\frac{1}{B^2}}{p^2+p\left(\frac{1}{Q}+\frac{QK}{A}\right)\frac{1}{B^2}+\frac{1}{B^2}} \qquad (3.26)$$

where: $B^2 = 1 + \frac{QKw}{Ax}$

Thus, our transfer function $\frac{V_2}{V_1}$ can be split into two sub-transfer functions such as:

$\frac{V_2}{V_1}$ = a * Delay Equalizer * Minimum Phase Network

$$= a * T_1(s) * T_2(s)$$

with:

$$T_1(s) = a\,\frac{p^2+p\left(\frac{1}{Q}+\frac{QK}{A}+QK\,\frac{a-1}{a}\right)\frac{1}{B^2}+\frac{1}{B^2}}{p^2-p\left(\frac{1}{Q}+\frac{QK}{A}+QK\,\frac{a-1}{a}\right)\frac{1}{B^2}+\frac{1}{B^2}} \qquad (3.27a)$$

$$T_2(s) = a\,\frac{p^2 - p\left(\frac{1}{Q} + \frac{QK}{A} + QK\,\frac{a-1}{a}\right)\frac{1}{B^2} + \frac{1}{B^2}}{p^2 + p\left(\frac{1}{Q} + \frac{QK}{A}\right)\frac{1}{B^2} + \frac{1}{B^2}} \qquad (3.27b)$$

Since the poles and zeros of the minimum phase network are very close to each other, its effect on the amplitude and delay responses of the all-pass section is very slight, Fig. 3.6. Comparing the results obtained with finite and infinite operational amplifier gain, we obtain:

$$w_{new} = \frac{w}{\left[1 + (wQK)/(Ax)\right]^{1/2}} = \frac{w}{F} \qquad (3.28)$$

$$Q_{new} = Q\left[1 + (wQK)/(Ax)\right]^{1/2} \qquad (3.29)$$

where:

$Q_{new} > 1/2$

$\frac{QK}{A} \ll 1$

F = Frequency correction factor.

3.7 Practical Example of an Active RC All-Pass Network of 8th Order.

The results obtained in section 3.6 were applied to realize the 8th order delay equalizer described in section 3.5 where " $Q = wC_1R_2$ ". The operational amplifier finite gain was chosen as $A = 10^6$, C_1 was made equal to C_2, and $R_B = 15$ KΩ. The element values and the new Q and w values are shown in Table 3.3. The delay and amplitude responses of

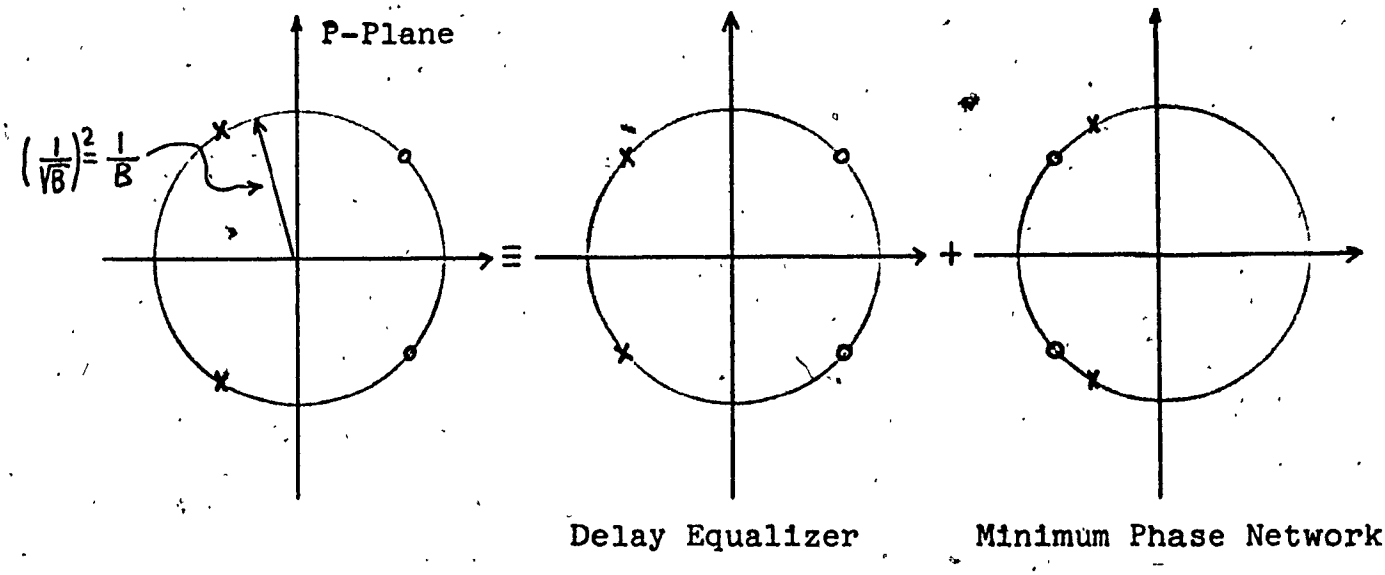

Fig. 3.6 Pole-Zero Pattern of "Bridgman & Brennan" Modified All-Pass Structure.

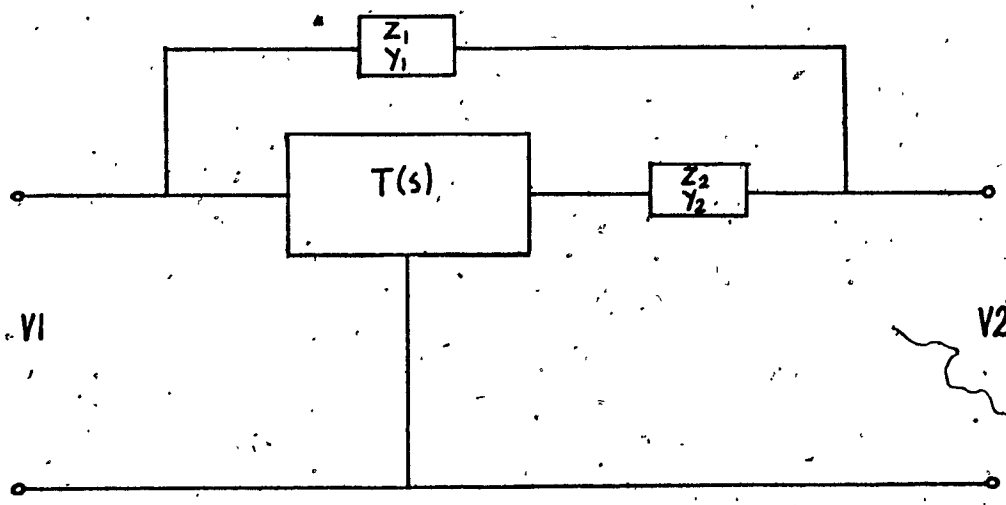

Fig. 3.7 All-Pass Network, "Bhattacharyya Configuration".

TABLE 3.3

ELEMENT VALUES USED IN 8th-ORDER RC DELAY EQUALIZER.

SECTION	F_o Hz.	F_{new} Hz.	Q	Q_{new}	C_1 PF.	C_2 PF.	R_1 Ω	R_2 Ω	R_b Ω	R_a Ω
1	1914	2023	4.89	4.62	10^4	10^4	850.5	72746.7	15000	701.5
2	2162	2316	5.46	5.10	10^4	10^4	674.0	70013.3	15000	577.6
3	2409	2624	6.15	5.65	10^4	10^4	536.9	68534.4	15000	470.0
4	2654	2936	6.70	6.06	10^4	10^4	447.3	65711.8	15000	408.4

Operational Amplifiers: 741C-MIL

R's : Vishay with .1% tolerances

C's : N.E. with 1% tolerances, polystirene.

the individual sections using RC-elements compared very closely to the ones obtained when RLC-elements were used, Table 3.2, with the exeption that with the RC-version amplitude losses of .397 db., .33 db., .27 db., and .23 db., were introduced in the four individual sections respectively, as expected from the term 20 log(1/a).

An error of approximately 5% was introduced when cascading the individual sections together, subsequently eliminated by the addition of three buffer amplifiers having an overall gain of approximately 1.23 db., thus offsetting the loss introduced by the four individual sections. Although the addition of these extra buffer stages appears as a drawback, this is greatly nullified by the fact that signals with prescribed loss or gain levels are normally required in practice, thus introducing the need for some extra amplifying stages.

The tuning of the circuit was rather straight forward and mainly necessary for the adjustment of the amplitude responses. The calculated values of R_2 required slight changes ($< 1\%$). This circuit, although requiring a slight longer time to adjust, appears to have definitely practical applications and possibly advantages over its LC-equivalent because of cost advantages introduced by the elimination of costly inductors and hermetical sealing. Note that to offset the error introduced by the amplifiers finite gains, the individual sections were tuned to higher frequencies F_{new}, as compared to the ideal values F_o, Table 3.3.

3.8 Effects of Finite Gain-Bandwidth Product of Operational Amplifiers.

In practical applications the gain-bandwidth product of operational amplifiers is finite, thus limiting the performance of active all-pass networks. In this section we will analize Genin's and Bhattacharyya's all-pass structures assuming the gain of the operational amplifier can be represented by " Ax/s+x ", as used in section 3.7.

3.8.1 Genin's All-Pass Configuration.

Referring to Fig. 2.5, we assume that no current flows into the inverting and non-inverting terminals. Also, if we take the voltage at the non-inverting terminal as being "V", then the potential at the inverting terminal is " $V-V_2d$ ", where: $d = 1/A_1$ and $A_1 = Ax/s+x$

For this circuit we have:

$$V_1 = (V/Z_2)Z_1 + V = V(1 + \frac{Z_1}{Z_2}) \qquad (3.30)$$

$$V_1 = (V - V_2d - V_2)\, R_1/R_f + V - V_2d \qquad (3.31)$$

From equations (3.30) and (3.31) we obtain:

$$V_1 = V_1 \frac{Z_2}{Z_1+Z_2}(1+\frac{R_1}{R_f}) - V_2\left[\frac{R_1}{R_f} + d(1+\frac{R_1}{R_f})\right]$$

$$V_1 = V_1 \frac{Z_2}{Z_1+Z_2}(1+B) - V_2\left[B + d(1+B)\right]$$

where: $B = R_1/R_f$

Rearranging, we get:

$$V_2\left[B + d(1+B)\right] = V_1 \frac{Z_2B-Z_1}{Z_2+Z_1} \qquad (3.32)$$

Thus: $$\frac{V_2}{V_1} = \frac{1}{B + d(1+B)} \frac{Z_2 B - Z_1}{Z_2 + Z_1} \qquad (3.33)$$

SPECIAL CASES

(1) Infinite Operational Amplifier Gain: $d \to 0$

$$R_f = R_1 \; ; \; B = 1$$

$$\frac{V_2}{V_1} = \frac{Z_2 - Z_1}{Z_2 + Z_1} \qquad (3.34)$$

(2) $d \to 0$

$$\frac{V_2}{V_1} = \frac{1}{B} \frac{Z_2 B - Z_1}{Z_2 + Z_1}$$

(3) $B = 1$ and $d = 1/A_1 = s+x/Ax$

$$\frac{V_2}{V_1} = \frac{1}{1+2d} \frac{Z_2 - Z_1}{Z_2 + Z_1} = \frac{1}{1+\frac{2(s+x)}{Ax}} \frac{Z_2 - Z_1}{Z_2 + Z_1}$$

$$= \frac{Ax}{2s+Ax+2x} \frac{Z_2 - Z_1}{Z_2 + Z_1} \simeq \frac{Ax}{2s+Ax} \frac{1 - Z_1 Y_2}{1 + Z_1 Y_2}$$

$$= \frac{Ax/2}{s+Ax/2} \frac{1 - Z_1 Y_2}{1 + Z_1 Y_2} = \frac{B}{s+B} \frac{1 - Z_1 Y_2}{1 + Z_1 Y_2} \qquad (3.35)$$

If we now take:

$$Y_2 = \frac{1}{sL_2} + sC_2 \quad \text{and} \quad Z_1 = R_1, \text{ then-}$$

$$\frac{V_2}{V_1} = - \frac{B}{s+B} \frac{s^2 - (s/C_2 R_1) + (1/L_2 C_2)}{s^2 + (s/C_2 R_1) + (1/L_2 C_2)} \qquad (3.36)$$

$$= - T_1(s) * T_2(s)$$

where:

$T_1(s)$ is the transfer function of a "Minimum Phase Network".

$T_2(s)$ is the ideal transfer function of a delay equalizer section.

For the "Minimum Phase Network" we have:

$$\left| T_1(s) \right|_{s-jw} = \left| \frac{B}{jw - B} \right| = \left| \frac{B}{(B^2 + w^2)^{1/2}} \angle -\tan^{-1}(w/B) \right| \qquad (3.37)$$

Over the voice frequency range, $f < 4KHz$, $B \gg w$, we obtain:

$$|T_1(s)| \approx |\angle -w/B| \text{ , since } \tan^{-1}(w/B) \approx w/B.$$

Also, for $\frac{w}{B} \ll 1$, the phase of T1(s) $= \phi$, where:

$$\phi = -\frac{w}{B} = \text{linear phase,}$$

and the delay "τ" is given by:

$\tau = \frac{d\phi}{dw} = \frac{1}{B}$, thus we see that the delay response is a constant, while the amplitude response is given by $|T_1(s)| \approx 1$.

This shows that the response of the "Minimum Phase Network" does not affect the relative value of the overall delay response. Also, the amplitude response remains practically constant over this frequency range, the loss being practically negligeable. As the frequency range is raised, the phase and delay responses become non-linear while the insertion loss increases slightly.

3.8.2 Bhattacharyya All-Pass Configuration.

Referring to Fig. 2.4, and breaking the circuit as shown in Fig. 3.7, we obtain:

$$\frac{V_2 - V_1}{Z_1} = \frac{TV_1 - V_2}{Z_2} = \frac{TZ_1 + Z_2}{Z_1 + Z_2} = T\left(\frac{Z_1}{Z_1 + Z_2}\right) + a$$

$$\frac{V_2}{V_1} = \left(T\,\frac{Z_1}{Z_2} + 1\right)a \quad ; \quad \text{where} \quad a = \frac{Z_2}{Z_1 + Z_2} \qquad (3.38)$$

The transfer function T(s) can be obtained from equation (3.33), letting $Z_1 = \infty$, $Z_2 = 0$, thus:

$$T(s) = -\frac{1}{B + d(1+B)} \qquad (3.39)$$

where:

$$d = 1/A_1, \quad A_1 = Ax/s+x, \quad B = R_1/R_f$$

The overall transfer function thus becomes:

$$\frac{V_2}{V_1} = \left(T\,\frac{Z_1}{Z_2} + 1\right) a$$

$$= \left(-\frac{1}{B+d(1+B)}\,\frac{Z_1}{Z_2} + 1\right) a$$

$$= \left(\frac{-Z_1+BZ_2+dZ_2(1+B)}{BZ_2+dZ_2(1+B)}\right) a = \left(\frac{(Z_2-Z_1) + 2dZ_2}{Z_2 + 2dZ_2}\right) a \Bigg|_{B=1}$$

$$\frac{V_2}{V_1} = \frac{(Z_2-Z_1) + 2Z_2/A}{(Z_2+Z_1)}\,\frac{Ax}{Ax+2s+2x} \qquad (3.40)$$

Thus, taking $1/Z_2 = sC2 + \frac{1}{sL_2}$ and $Z_1 = R_1$, we see that the same conclusions as explained for Genin circuit apply to Bhattacharyya all-pass configuration as the term "$\frac{2Z_2}{A}$" approaches zero. If this was not true, the poles and zeros of our transfer function would have slight different Q's and would lie on circles of different radii, thus destroying the all-pass function requirement for zeros and poles being mirror images of each other, resulting in a distorted all-pass function for frequencies near "w".

3.9 Comparison Figures For Second Order All-Pass Networks.

A summary of the all-pass structures investigated in this major technical report is shown in Table 3.4. The first three configurations(No. 1,2,3), which were not fully investigated in this report, are slightly more complex than the last three(No. 4,5,6). Both Yanagisawa and Bobrov realizations exhibit control of the poles and zeros by varying the "NIC" and amplifiers gains respectively, while enabling compensation for input and load impedances.

In this report, the one operational amplifier circuits (Configurations No. 4,5,6) have been analyzed more extensively because of their simplicity and minimum number of components, thus making them more attractive for low quantity production using discrete components. Both Genin and Bhattacharyya configurations were shown to be equivalent, Genin's circuit having a slight higher input impedance "$Z_{11} = Z_1 + Z_2$"($R \to \infty$ in Fig. 2.4 and Fig. 2.5) as compared to Bhattacharyya circuit having an input impedance of "$Z_{11} = 5/6(Z_1 + Z_2)$", thus introducing slight smaller errors in the overall delay and amplitude responses of cascaded second order all-pass sections. Occasionally, isolation amplifiers are introduced between sections to eliminate any possibility of error while introducing a specified gain in the overall network response. Both these circuits were limited to real poles and zeros realizations when used strictly with RC elements, Configuration No.5.

The all-pass nature of both circuits remained unchanged when the responses were analyzed with finite operational amplifier gains, the overall network responses being equivalent to the responses of an ideal all-pass section cascaded with a minimum-phase section.

Configuration No. 6 shows the realization of a second order all-pass network with real or complex poles and zeros using one operational amplifier and strictly RC elements. This circuit, when analyzed with finite operational amplifier gain, behaved similarly to Genin and Bhattacharyya circuits, the errors introduced in the "w" and "Q" values being negligeable if " $wQK/Ax \ll 1$". Also, although this circuit is more difficult to adjust than Configuration No. 5 (using RLC elements), it appears to have definitely practical applications and possibly advantages over its RLC equivalent because of cost advantages introduced by the elimination of costly inductors and hermetical sealing,

TABLE 3.4

COMPARISON FIGURES FOR SECOND ORDER ALL PASS NETWORKS

NO.	CONFIGURATION	NUMBER OF				R_{max}/R_{min}	C_{max}/C_{min}	Q with O.A. GAIN $\rightarrow \infty$	Q with FINITE O.A. GAIN
		R	C	L	O.A.				
1	YANAGISAWA (Fig.1.4)	3	3	-	1	2(1+d)	2(1+d)	w/2d	-
2	LOVERING (Fig.1.6)	6	4	-	2	2w(1+d)	2(1+d)	w/2d	-
3	BOBROV (Fig.1.7)	3	3	-	2	2(1+d)	4	w/2d	-
4	GENIN and BHATTACHARYYA (Fig.2.4)	2	2	-	1	1	1	1/3	Same(All-Pass cascaded with Min. Phase Network)
5	GENIN and BHATTACHARYYA (Fig.2.5)	1	1	1	1	-	-	$R1(C2/L2)^{1/2}$	"
6	BRIDGMAN and BRENNAN"Mod." (Fig.3.5)	4	2	-	1	$\frac{2Q^3}{wCR_b} = \frac{R2}{R_a}$	1 (C1=C2)	$\frac{1}{2}\left(\frac{R2}{R1}\right)^{1/2}$	$Q_{new}=Q\left(1+\frac{wQK}{Ax}\right)^{1/2}$

NOTES 1. For Configurations No. 1,2,3, the transfer function is: $s^2-2dws+w^2/s^2+2dws+w^2$ where: d= Damping Factor = $w/2Q < 1$.

2. For Configuration No. 4: $Z1= R + 1/Cs$; $(Z2)^{-1} = 1/R+Cs$; $B=R_i/R_f = 5$.

3. For Configuration No. 5: $Z1=R1$; $(Z2)^{-1} = sC2 + 1/sL2$; $B=R_i/R_f = 1$.

4. O.A. = Operational Amplifier.

CONCLUSION

In this report we have shown that active all-pass networks with the required delay, phase, and amplitude characteristics can be easily achieved, as it is clearly indicated by their use in recently designed telephone communication equipment. These networks find their greatest applications at relatively low frequencies where their much smaller sizes and costs, and better response characteristics than their passive equivalents make their use very attractive.

In one application, gyrators were used for the simulation of inductors required for the realization of a 4^{th} order all pass transfer function. Although the operational amplifiers used to realize the gyrators were internally compensated, external compensation is preferable so as to optimize the gyrator bandwidth. For optimun gyrator realizations, operational amplifiers with high "low frequency gain" ($\geq$60 db.), large 3-db. bandwidth ($\geq$50 KHZ.), and freedom from latch-up are required, and as they are not easily obtainable commercially, most applications require special custom-made realizations for frequencies in the range of 25 KHz. and up.

We have also seen that all-pass transfer functions with either real or complex poles and zeros can be equally realized using single operational amplifiers and either RLC or RC elements. Designs using "minimum sensitivity" with respect to the operational amplifier gain showed amplitude response improvement, especially over temperature variations from $0^{o}C$ to $50^{o}C$.

The main disadvantages of active all-pass networks are the need for external power sources and the limitations to frequencies below a few hundred kilocycles. Nevertheless, as time goes on, these limitations will be overcomed by the development of differential input operational amplifiers with high common mode rejection ratios, improved gain-bandwidth products, and lower power consumption.

Although this investigation was mainly restricted to realizations with discrete RLC elements and single operational amplifiers, other very stable versions of all-pass structures can be realized using a larger number of operational amplifiers[18,19] and taking advantage of new technology findings such as "Hybrid Integrated Circuits"[20] and "Distributed RC Networks"[21].

REFERENCES

1. H.Matthes,"Designing high grade delay equalizers", UDC 621.372.553: 621.399.74 (1965) pp. 177-185.
2. U.S.Ganguly,"On inductorless all-pass phase shifter", IEEE Proceedings, October 1966, pp. 1462-1463.
3. R.Genin,"Realization of an all-pass transfer function using operational amplifiers", Proc. IEEE (letters), vol. 56, pp. 1746-1747, October 1968.
4. B.B.Bhattacharyya,"Realization of an all-pass transfer function", Proc. IEEE (letters), vol. 57, pp.2092-2093, November 1969.
5. S.C.Dutta Roy,"RC-active all-pass networks using a differential input operational amplifier", Proc. IEEE (letters), vol 57, pp. 2055-2056, November 1969.
6. R.W.Calfee,"On active network equivalent to the constant resistance lattice with delay circuit applications", IEEE Transactions on Circuit Theory, vol. CT-10, pp. 532-533, December 1963.
7. T.Yanagisawa,"RC active networks using current inversiion type negative-impedance converters", IRE Trans., CT-4, 140(1957).
8. W.F.Lovering,"Analog computer simulation of transfer function", Proc. IEEE, 53, 306(March 1965).
9. L.S.Bobrov,"On active RC synthesis using an operational amplifier", Proc. IEEE, 53,1648-1649 (October 1965).

10. S.K.Mitra,"Analysis and synthesis of linear active networks", John Wiley & Sons, Inc., New York, 1969.

11. B.B.Bhattacharyya and M.N.S.Swamy,"Active RC all-pass networks with a grounded operational amplifier", Proc. IEEE(letters), pp. 933, June 1970.

12. A.Antoniou,"Realization of gyrators using operational amplifiers, and their use in RC-active network synthesis", Proc. IEEE, vol. 116, No. 11, November 1969.

13. H.J. Orchard,"Inductorless bandpass filters", IEEE-Journal of Solid-State Circuits, vol. SC-5, No.3, June 1970.

14. S.C.Dutta Roy,"On inductor simulation using a unity gain amplifier", IEEE Journal of Solid-State Circuits, Vol.SC-5, No. 3, pp. 95-98, June 1970.

15. B.B.Bhattacharyya and M.N.S.Swamy,"On the realization of an all-pass or a notch filter", Proc. IEEE, 58, 4, pp. 603-604, April 1970.

16. I.M.Horowitz,"Optimazation of negative-impedance conversion methods of active RC synthesis", IRE Trans. Circuit Theory, vol. CT-6, pp. 296-303, Sept. 1959.

17. G.E.Roberts,"On tuning the group delay of an active RC all-pass resonator," IEEE Trans. Circuit Theory, pp. 172-173, March 1973.

18. J.Tow,"A step-by-step active filter design", IEEE Spectrum, pp. 64-68, December 1969.

19. J.Tow,"Design formulas for active RC filters using operational amplifier biquad", Electronic Letters, pp. 339-341, July 24, 1969.

20. G.S.Moschytz and W.Thelen,"Design of hybrid integrated filter building blocks", IEEE Journal of Solid-State Circuits, vol. SC-5, NO. 3, June 1970.

21. N.Sen Roy," Realization of all-pass characteristics utilizing a distributed RC network," Proc. IEEE(letters), pp. 1235-1236, October 1972.